Supporting Information

The strong antibacterial properties of anion transporters: a result of depolarization and weakening of the bacterial membrane

Claude-Rosny Elie, Guillaume David and Andreea-Ruxandra Schmitzer*

Departement de Chimie, Universite de Montreal, CP 6128 Succursale Centre Ville, H3C 3J7 Montreal, Quebec, Canada. Correspondence should be addressed to A.R.S (ar. schmitzer@umontreal.ca)

Table of contents

NMR and MS spectra

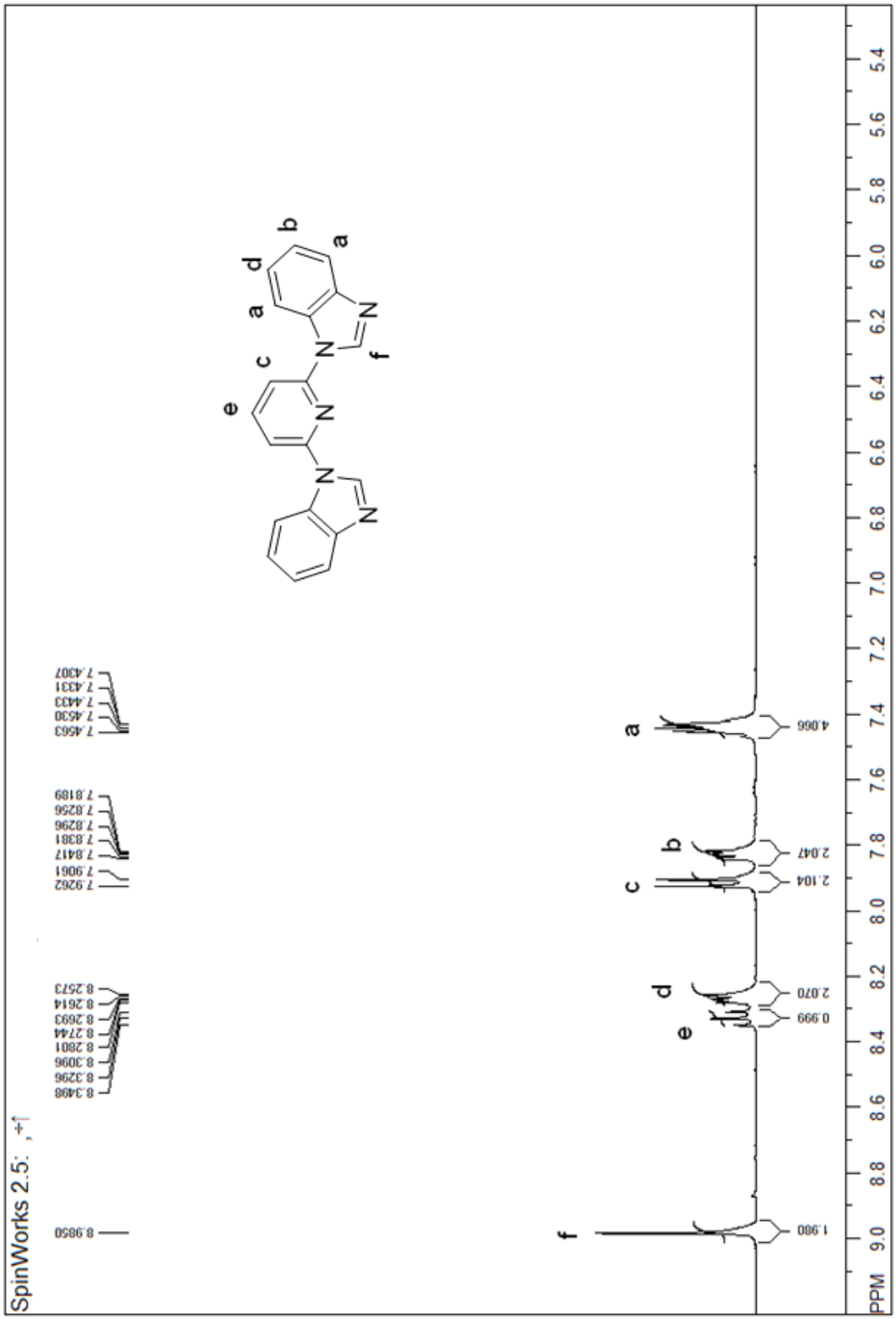

Supplementary figure S1. ^{1}H NMR (CD_3OD) spectrum of 2,6-bis(1H-benzo[d]imidazol-1-yl)pyridine.

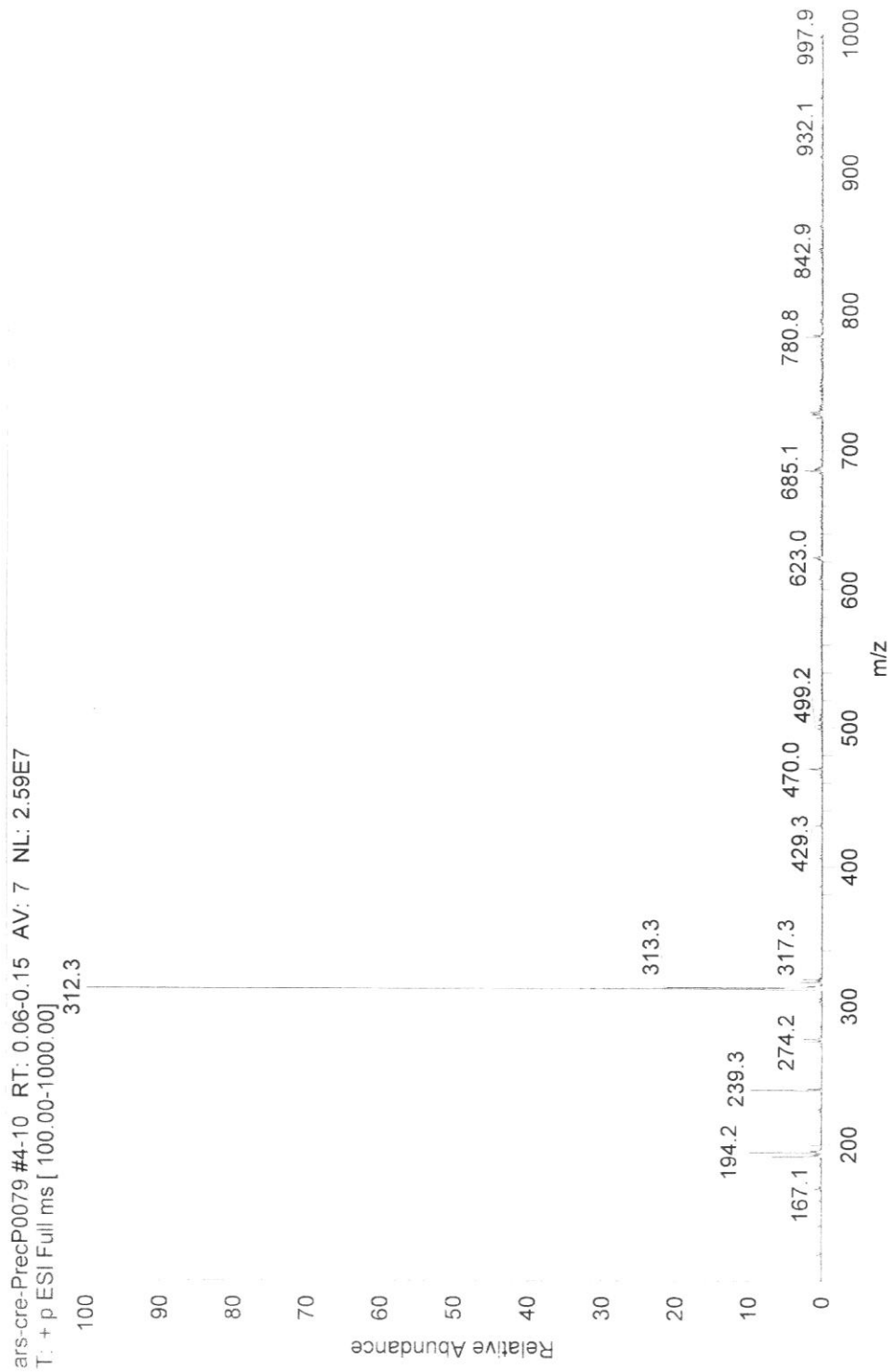

Supplementary figure S2. ESI mass spectrum (positive ionization) of 2,6-bis(1H-benzo[d]imidazol-1-yl)pyridine.

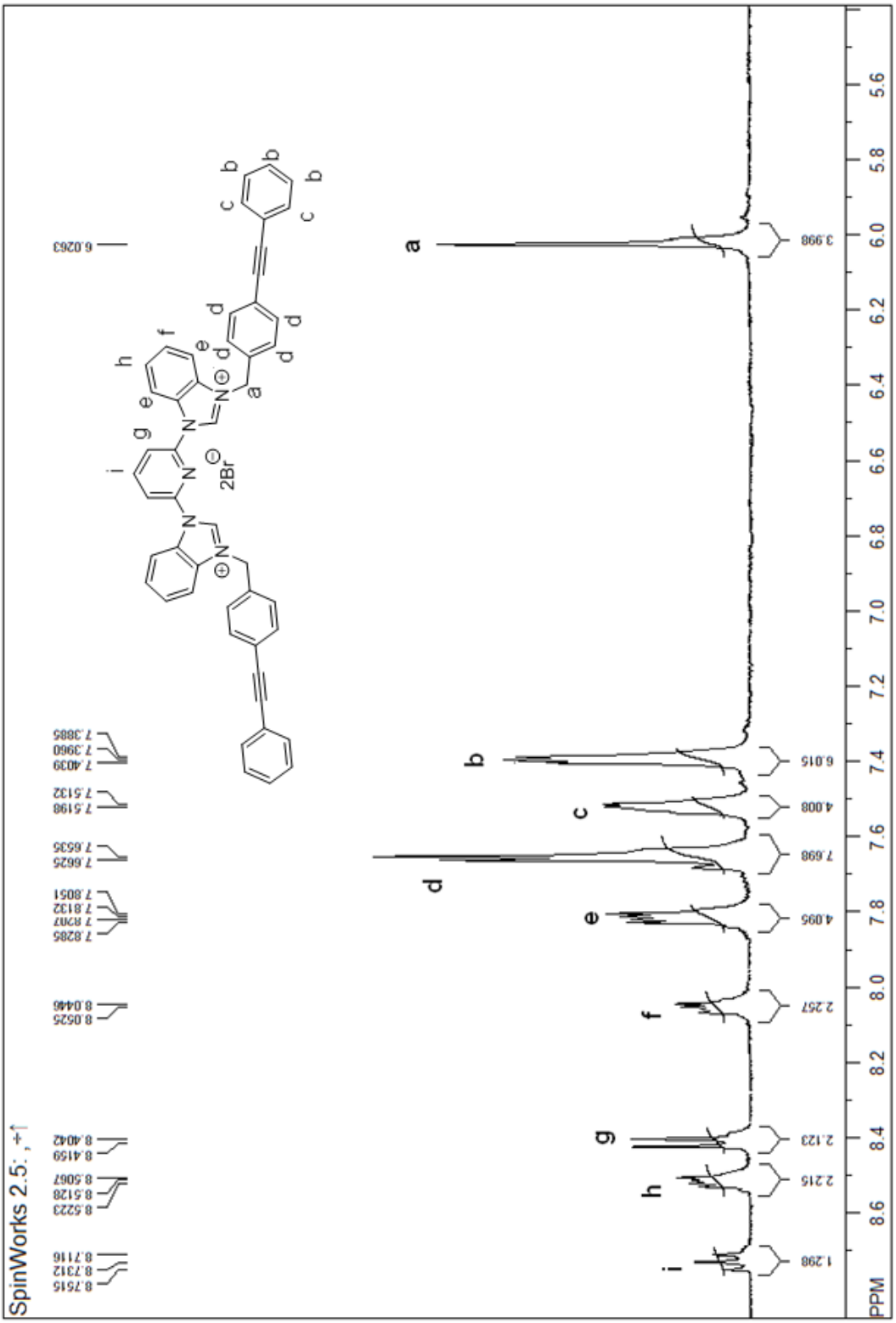

Supplementary figure S3. ^{1}H NMR (CD_3OD) spectrum of **3**.

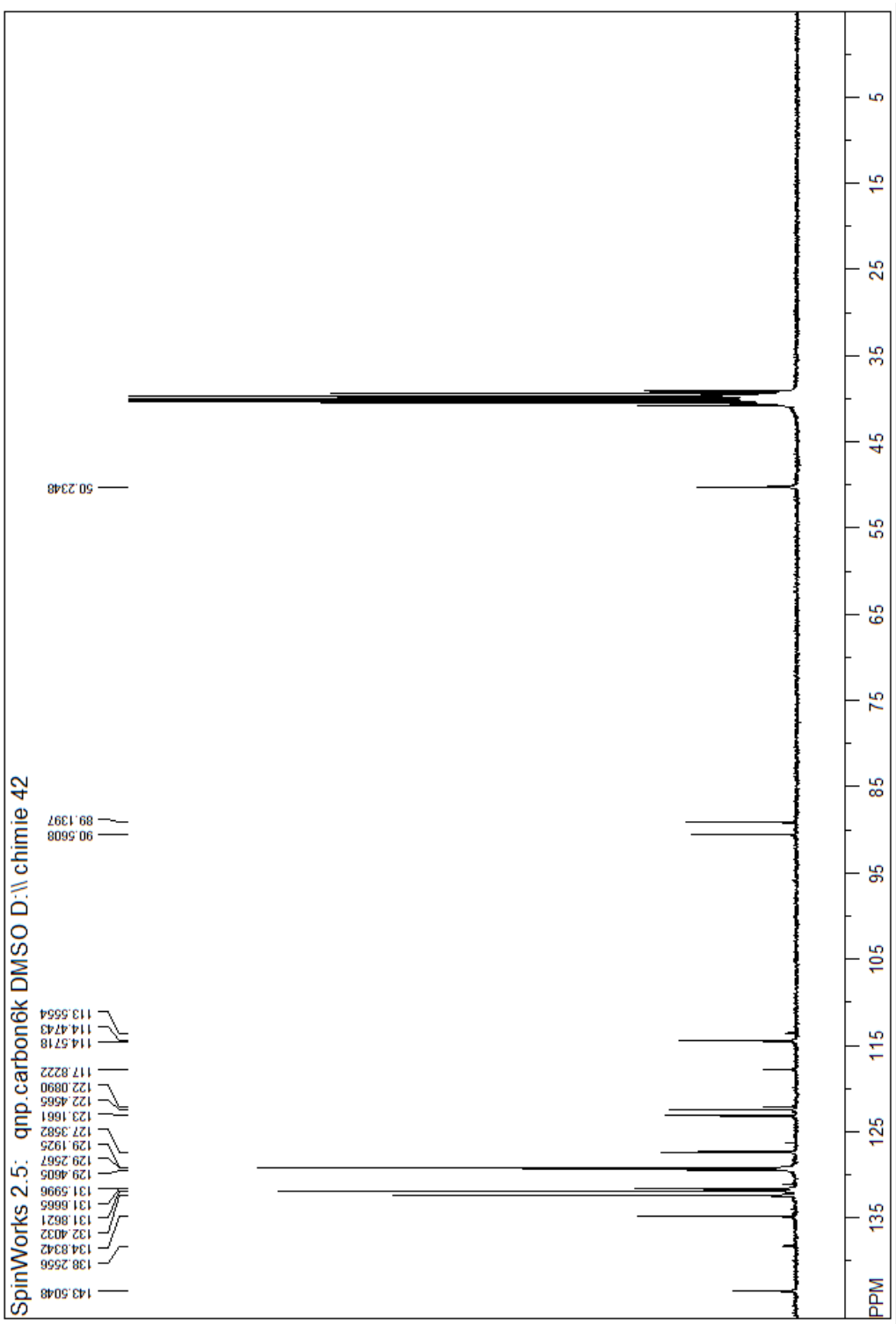

Supplementary figure S4. ^{13}C NMR (DMSO-d_6) spectrum of **3**.

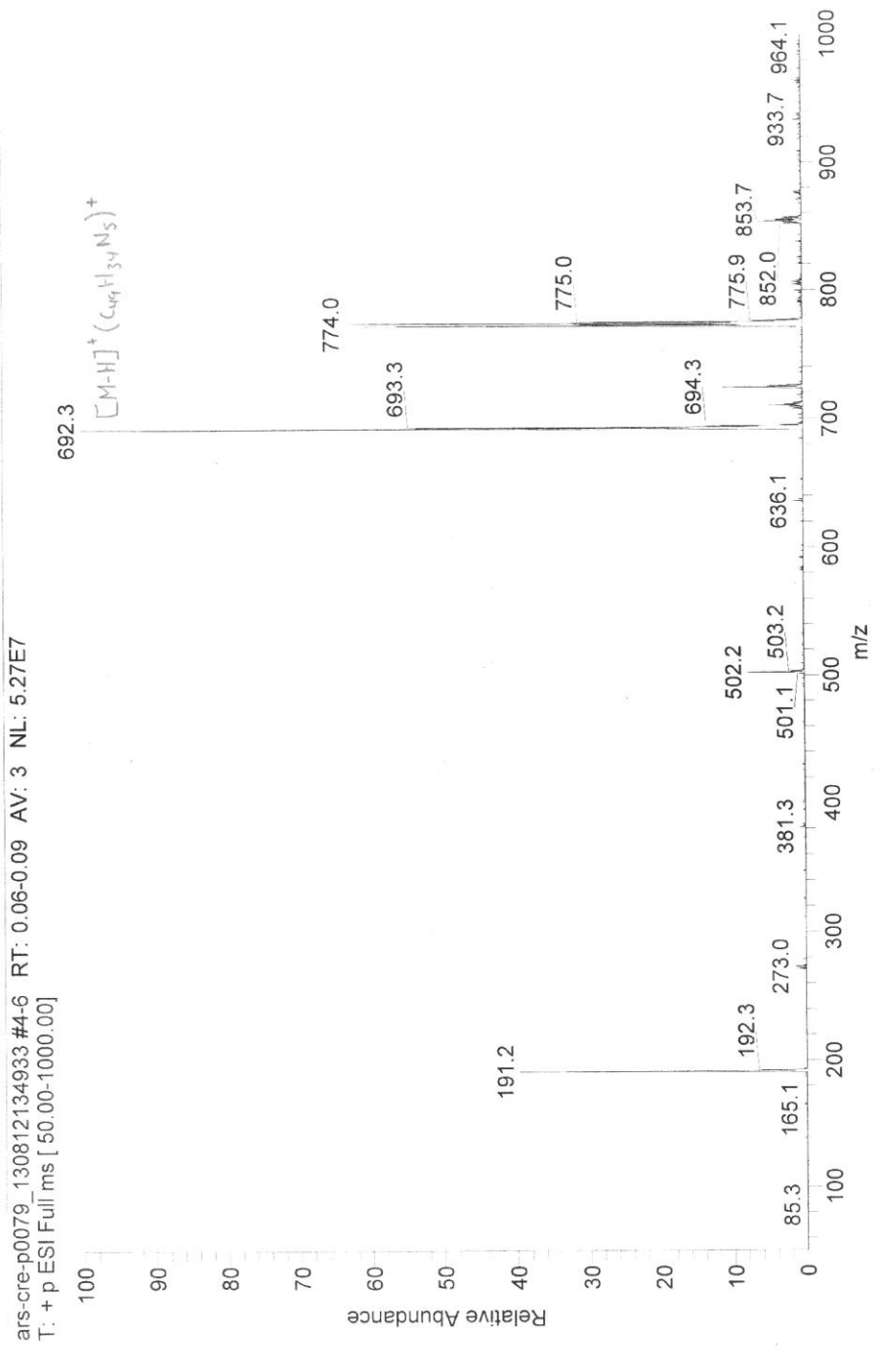

Supplementary figure S5. ESI mass spectrum (positive ionization) of **3**.

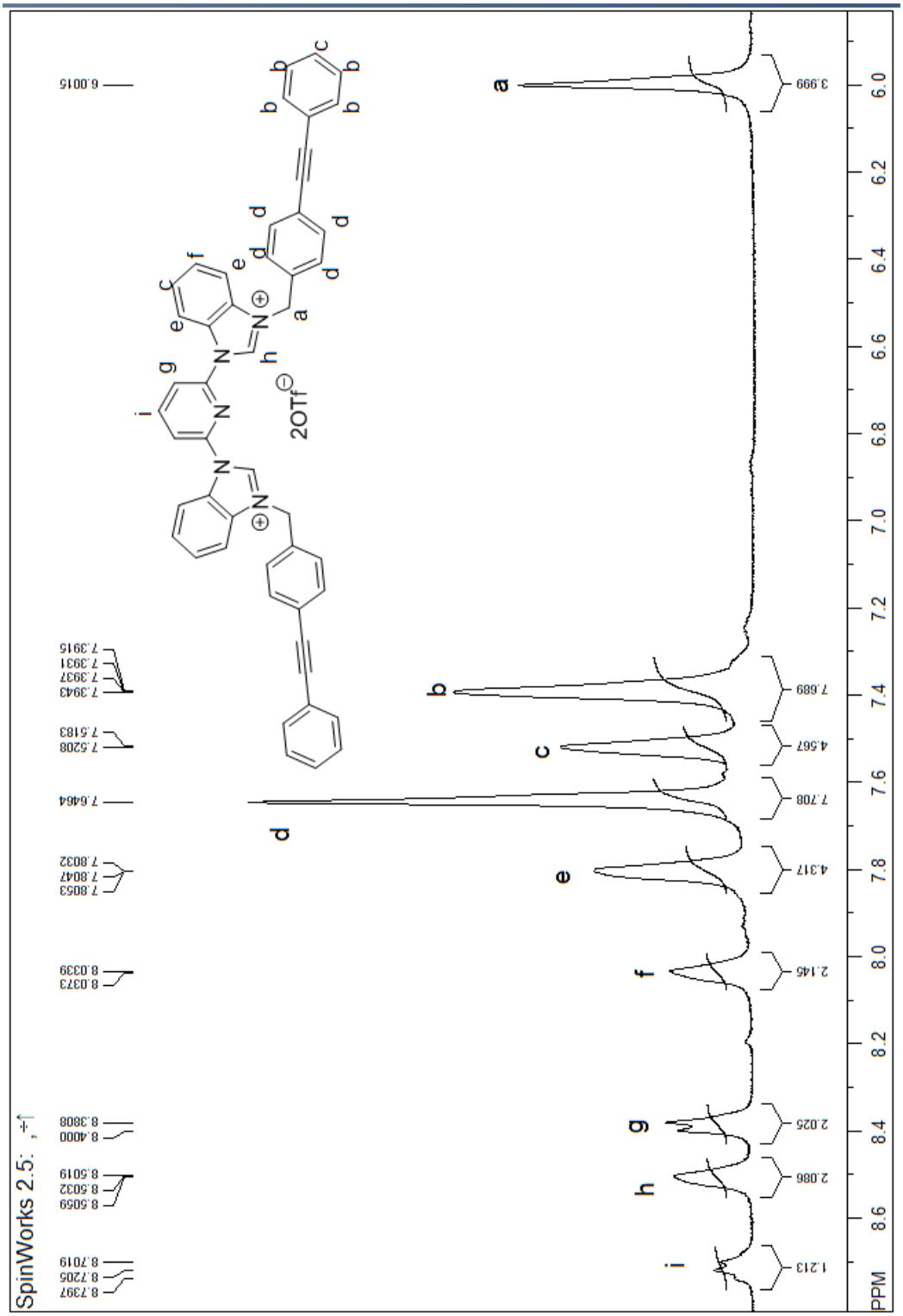

Supplementary figure S6. ^{1}H NMR (CD_3OD) spectrum of **5**.

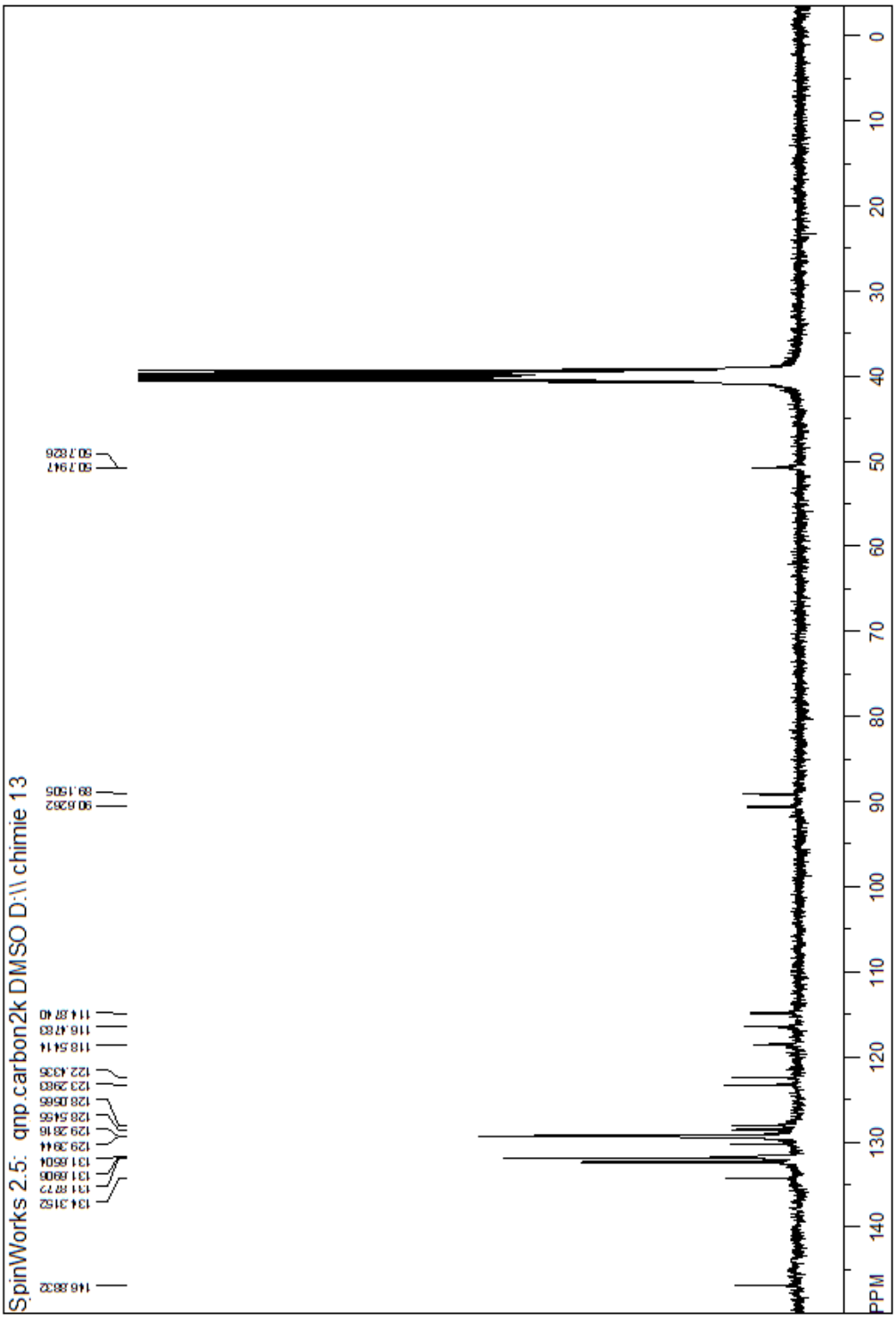

Supplementary figure S7. ^{13}C NMR (DMSO-d_6) spectrum of **5**.

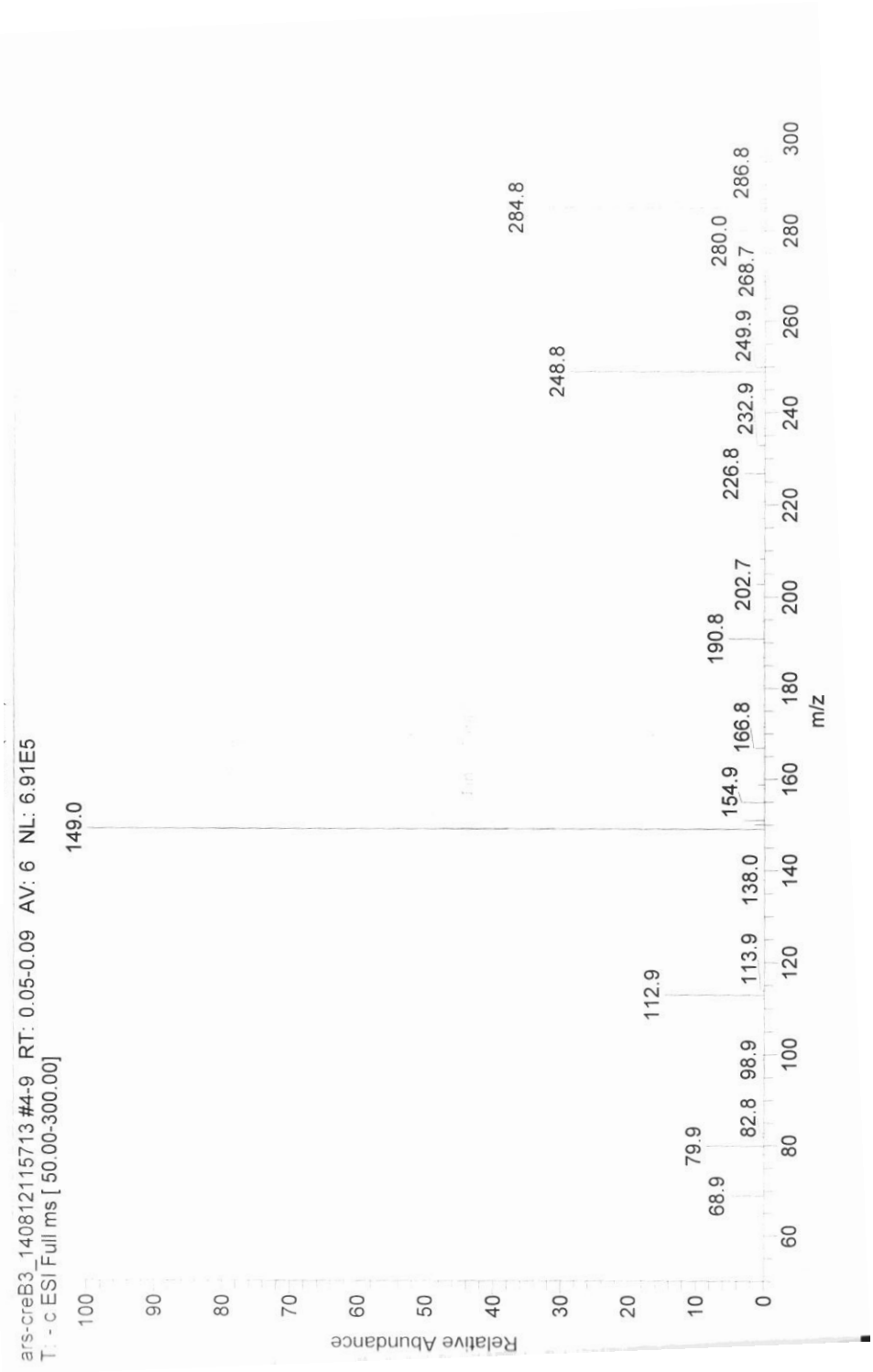

Supplementary figure S8. ESI mass spectrum (negative ionization) of **5**.

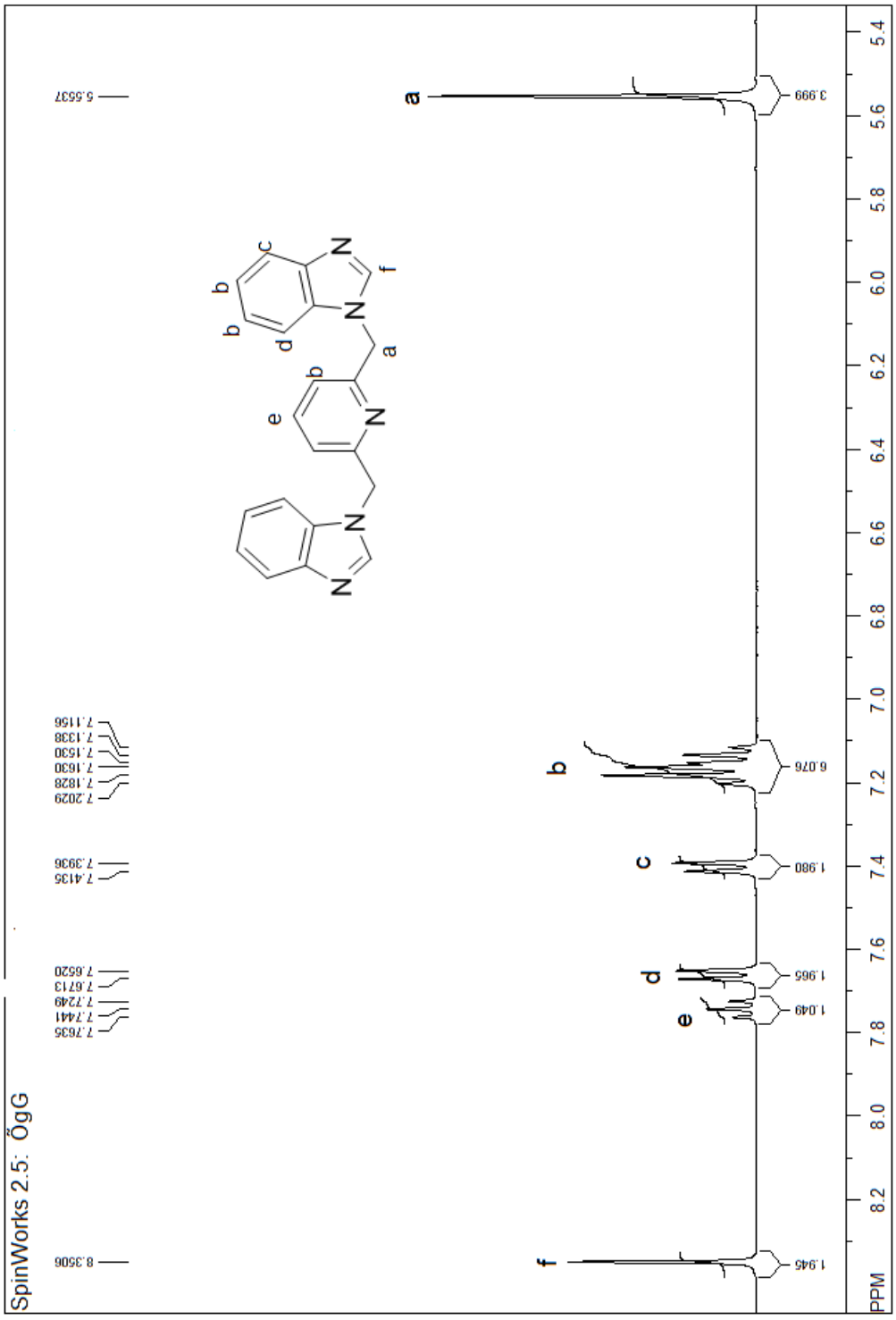

Supplementary figure S9. ^{1}H NMR (CD_3OD) spectrum of 2,6-bis((1H-benzo[d]imidazol-1-yl)methyl)pyridine.

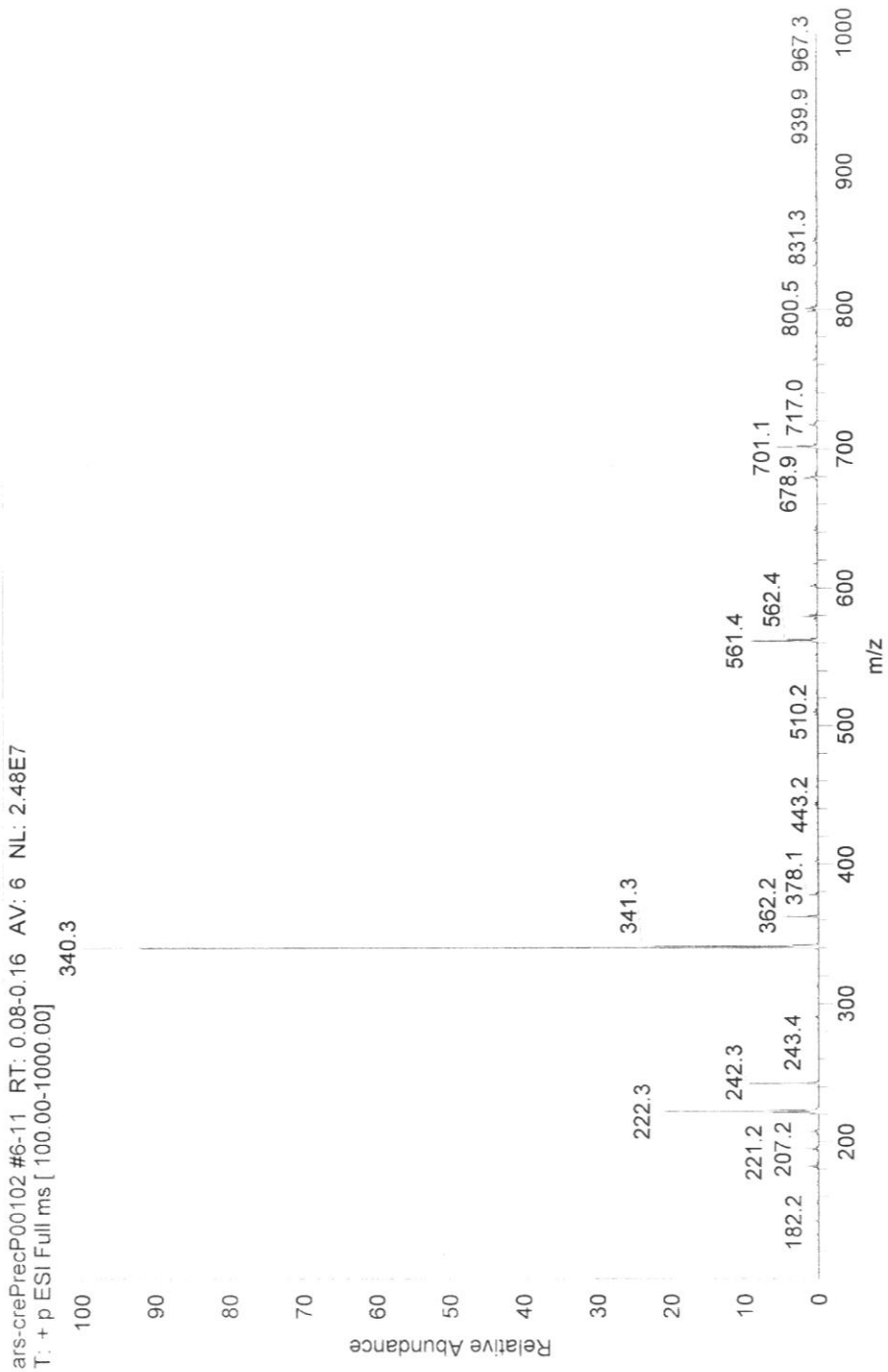

Supplementary figure S10. ESI mass spectrum (positive ionization) of 2,6-bis((1H-benzo[d]imidazol-1-yl)methyl)pyridine.

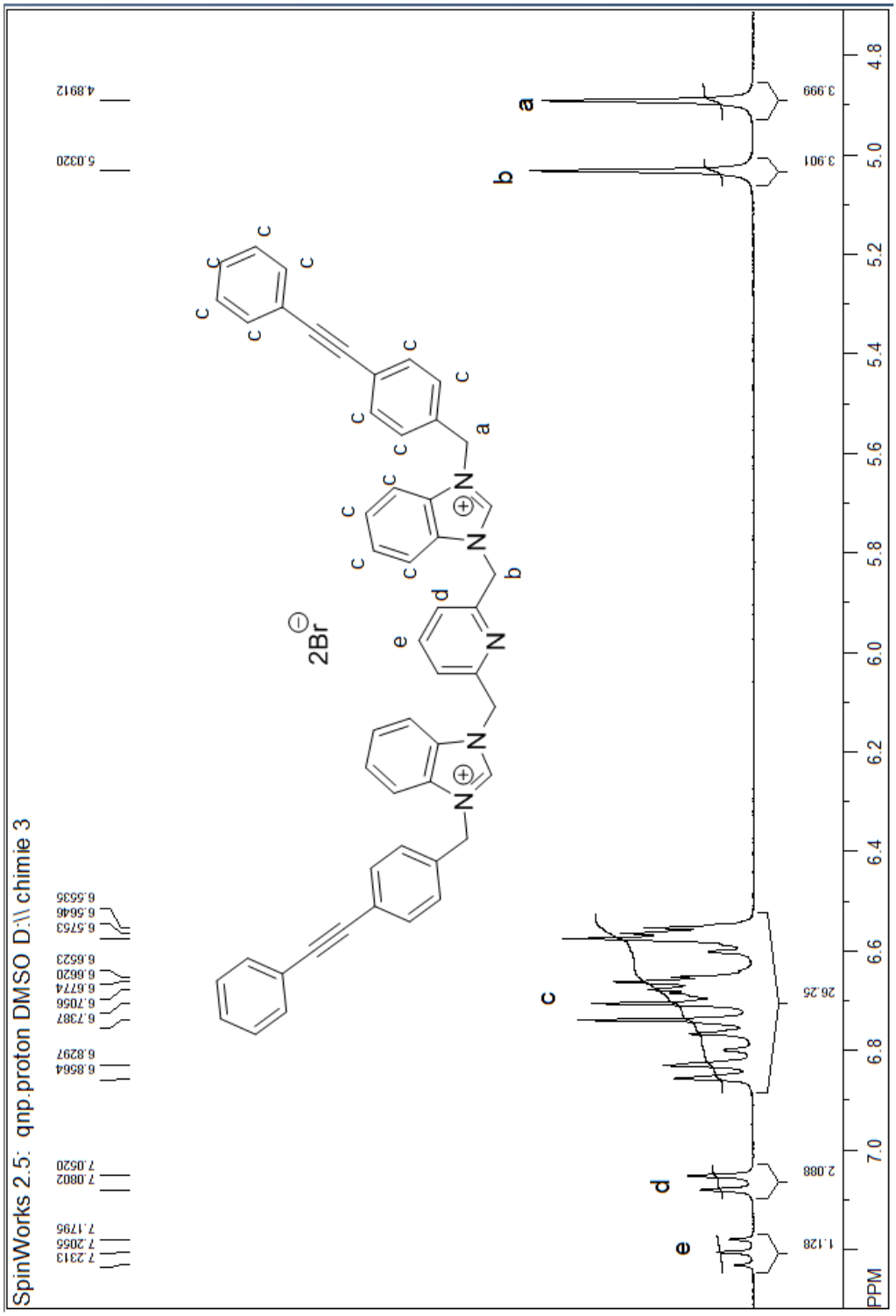

Supplementary figure S11. ^{1}H NMR (CD_3OD) spectrum of **6**.

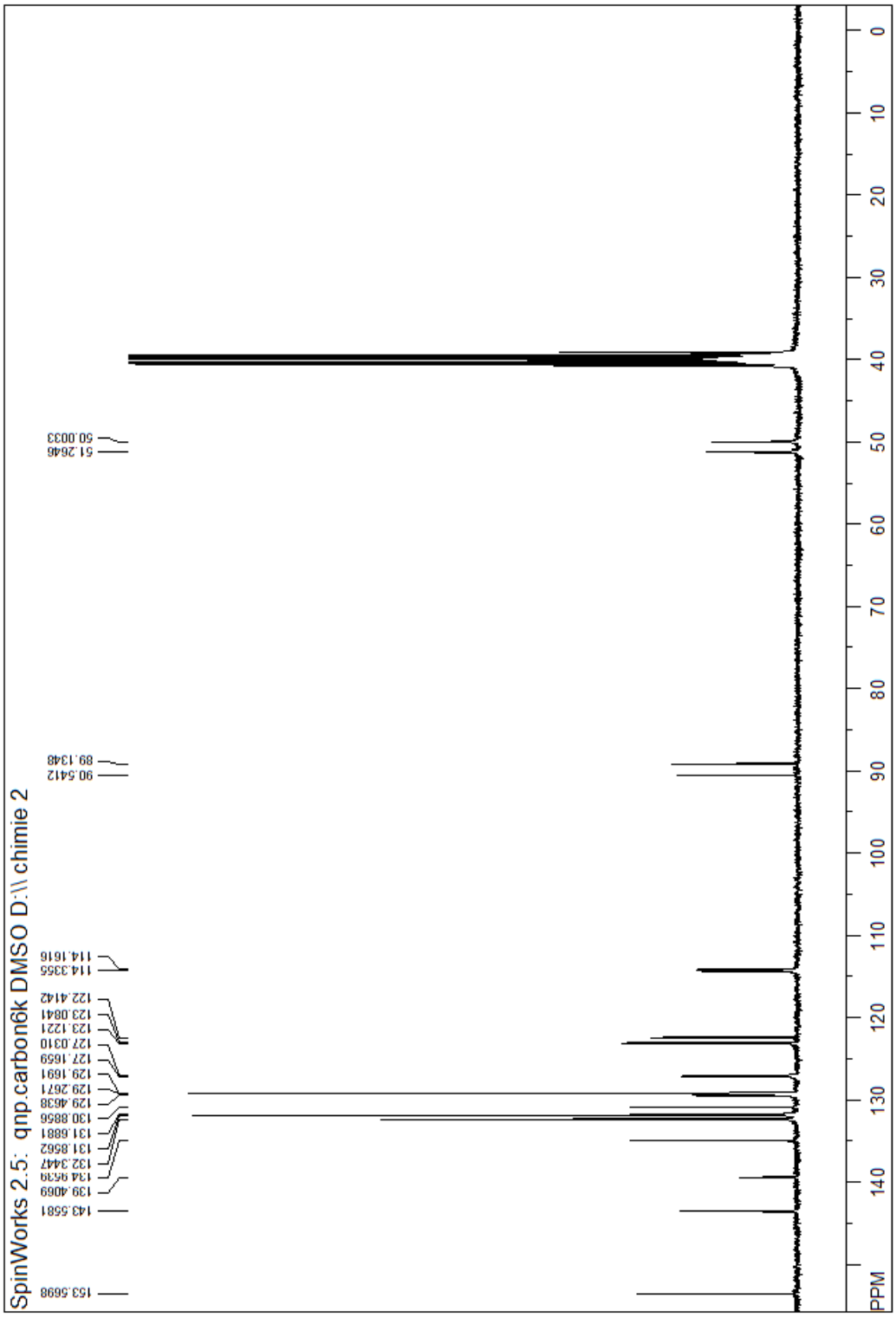

Supplementary figure S12. ^{13}C NMR (DMSO-d_6) spectrum of **6**.

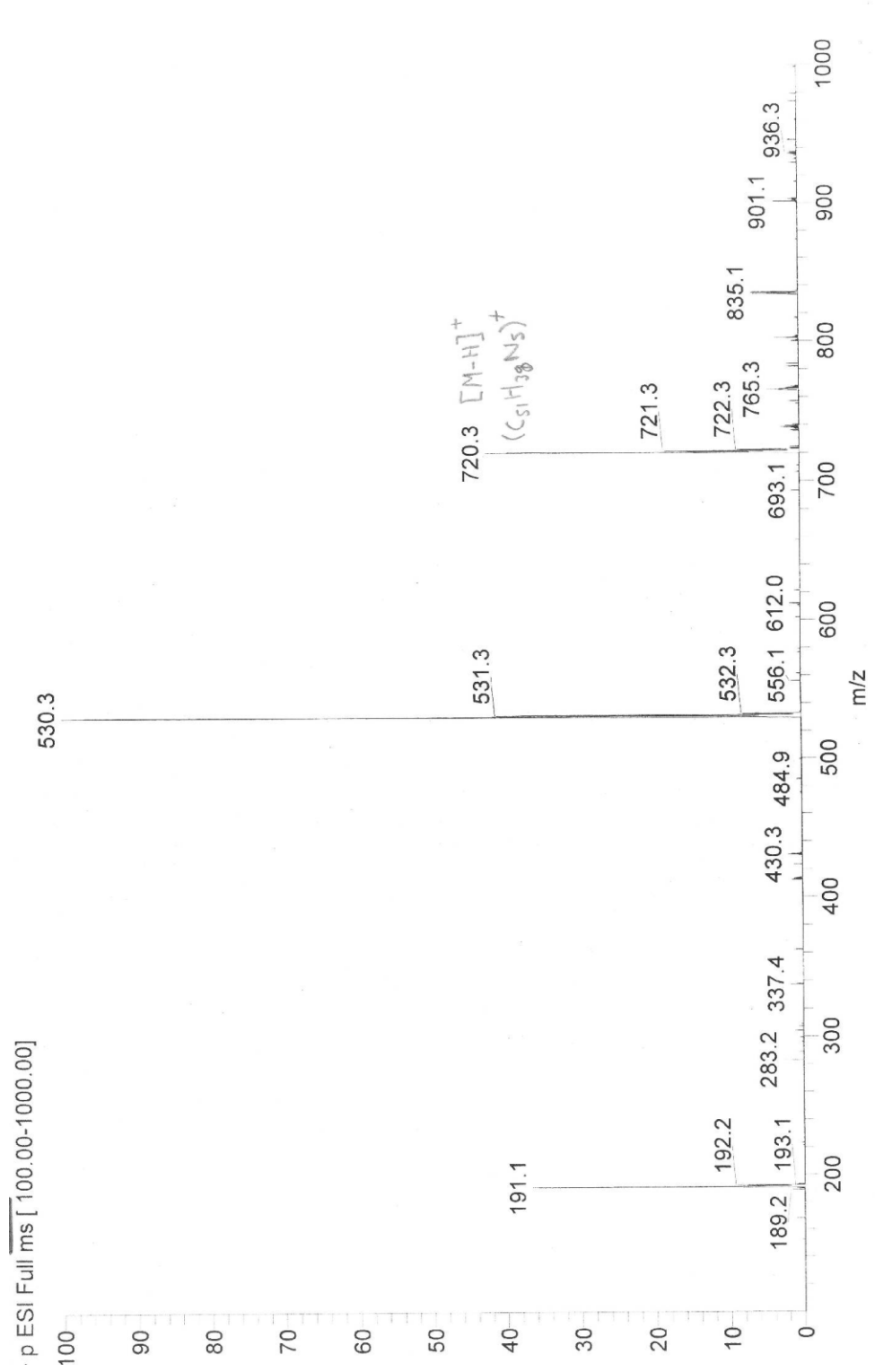

Supplementary figure S13. ESI mass spectrum (positive ionization) of **6**.

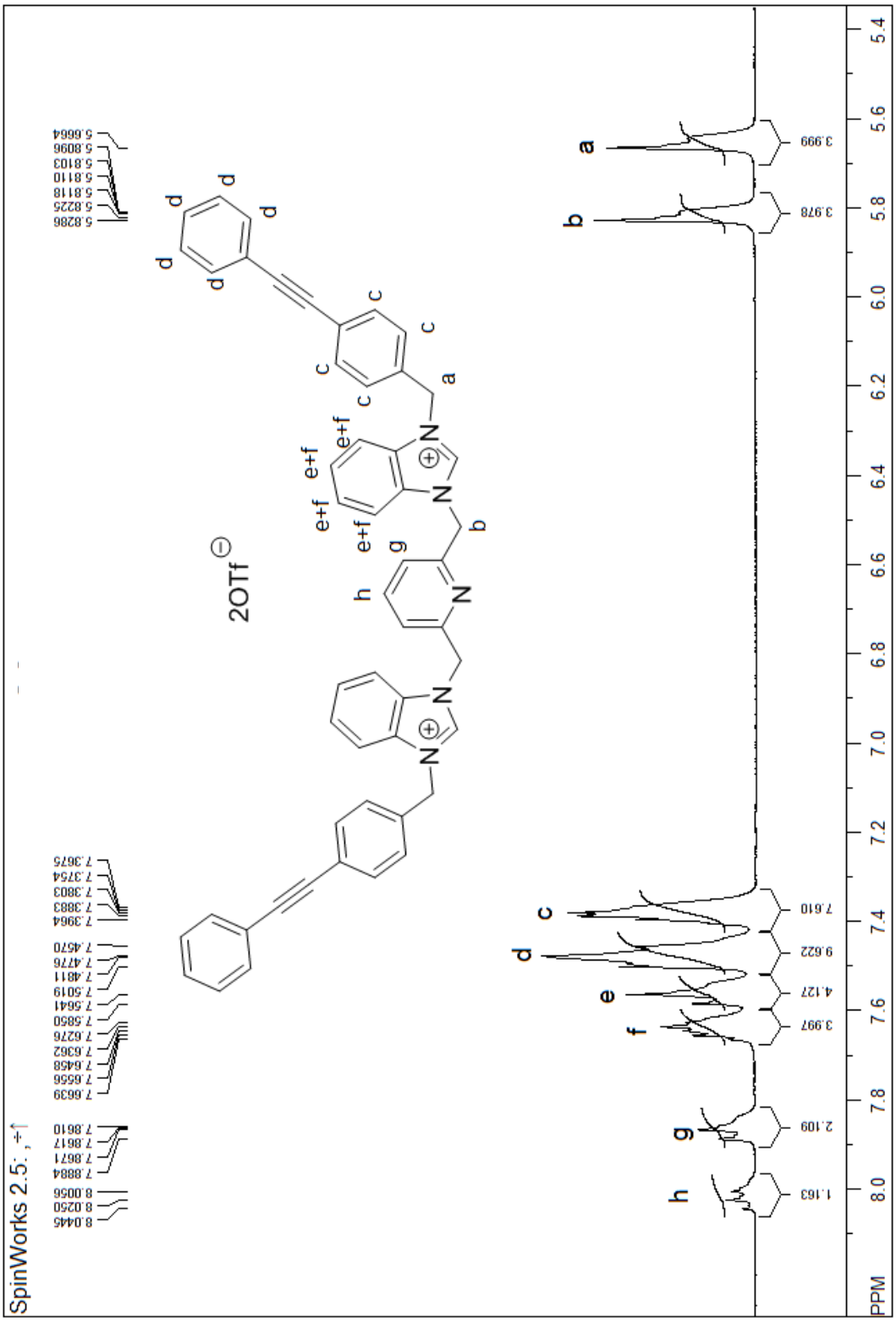

Supplementary figure S14. ^{1}H NMR (CD_3OD) spectrum of **8**.

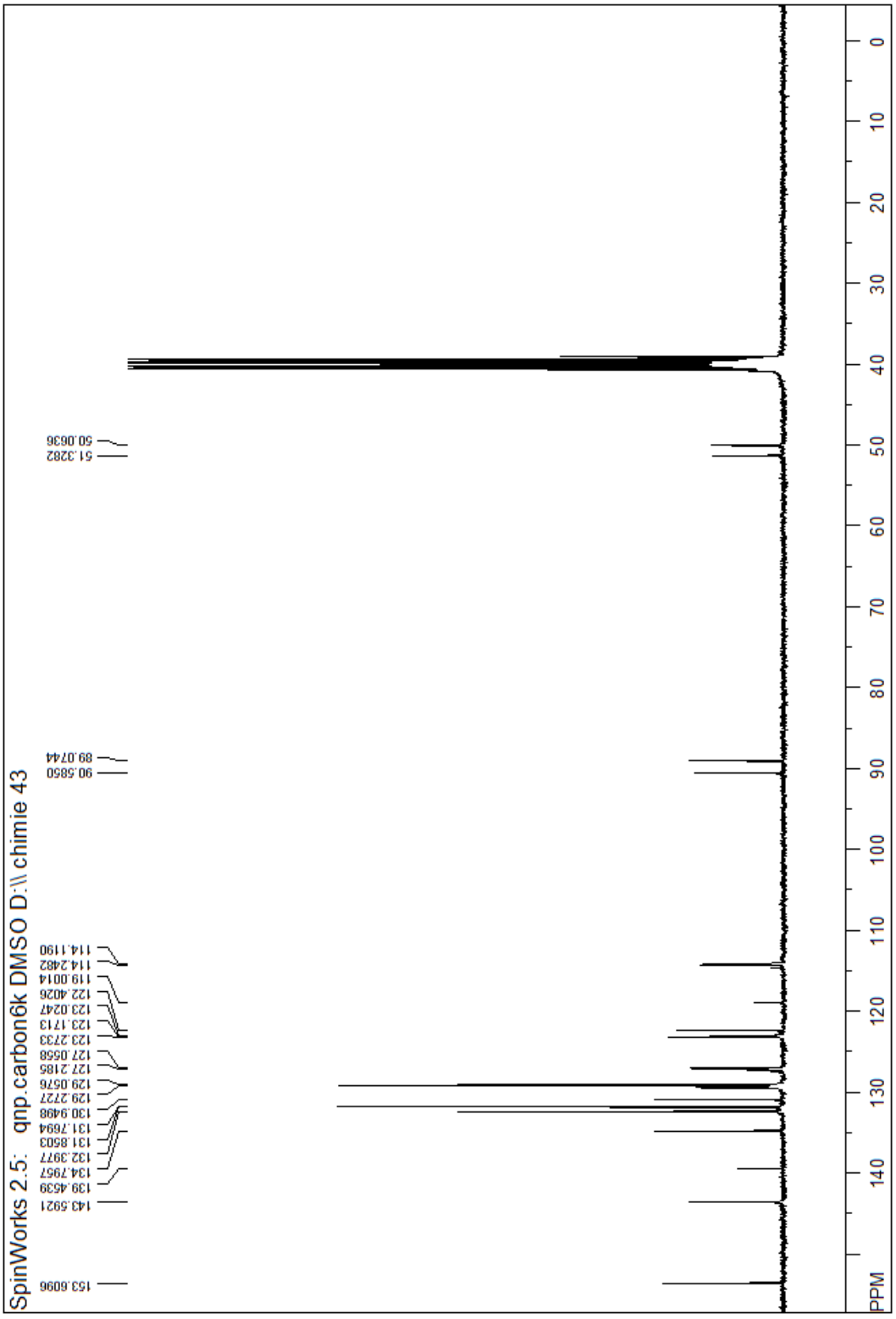

Supplementary figure S15. ^{13}C NMR (DMSO-d_6) spectrum of **8**.

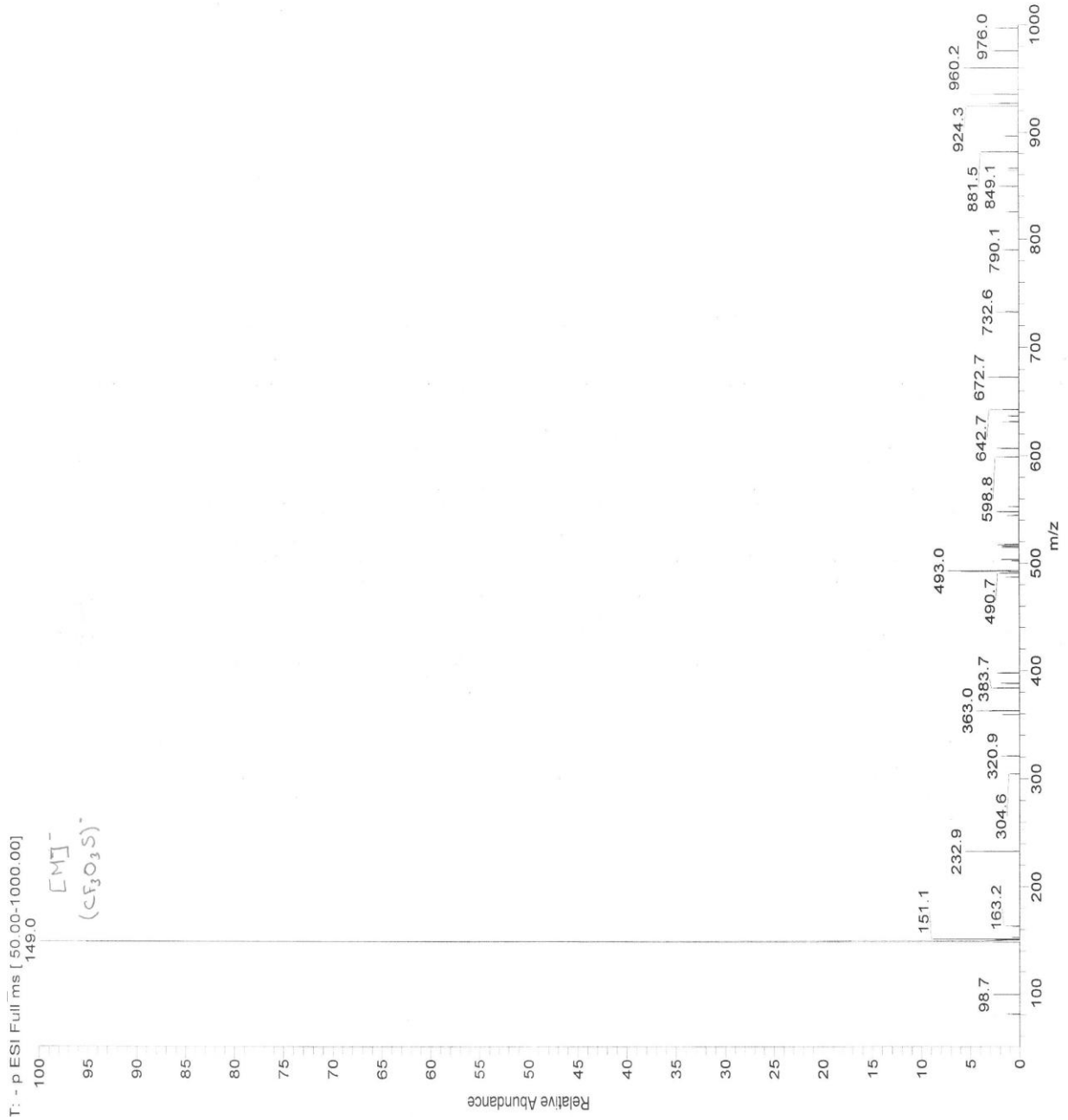

Supplementary figure S16. ESI mass spectrum (negative ionization) of **8**.

Anion transport assays in DPPC and EYPC liposomes

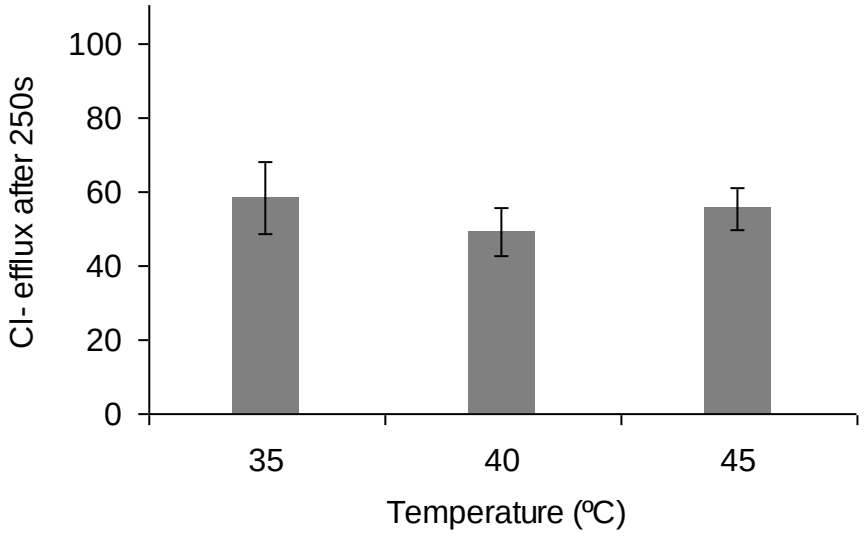

Supplementary figure S17. Chloride efflux out of DPPC liposomes at 35 °C, 40 °C and 45 °C. The data at each temperature are obtained by using 10 mol% of benzimidazolium salt **1** (relative to DPPC concentrations). The data at each temperature are the average of three series of measurements.

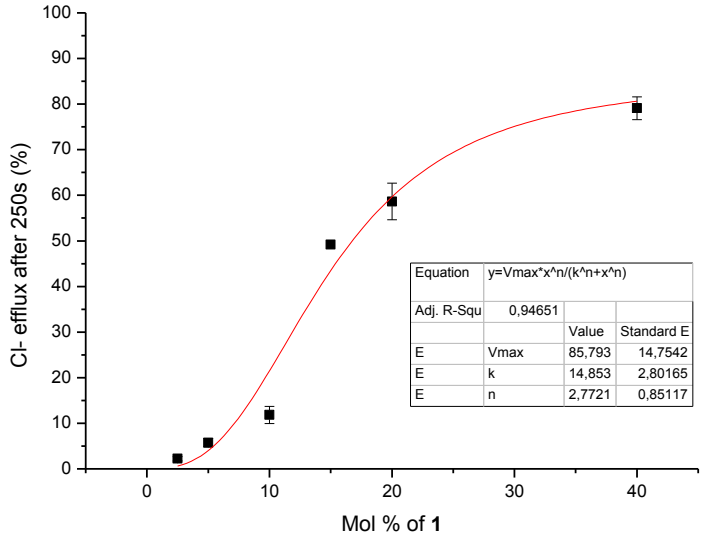

Supplementary figure S18. Hill plot for chloride release mediated by compound **1** from EYPC LUVs loaded with 100 mM NaCl buffered to pH 6.4 with 10 mM phosphate buffer. The vesicles were dispersed in 100 mM $NaNO_3$ buffered to pH 6.4 with 10 mM phosphate buffer. Chloride efflux was measured 250 s after injection.

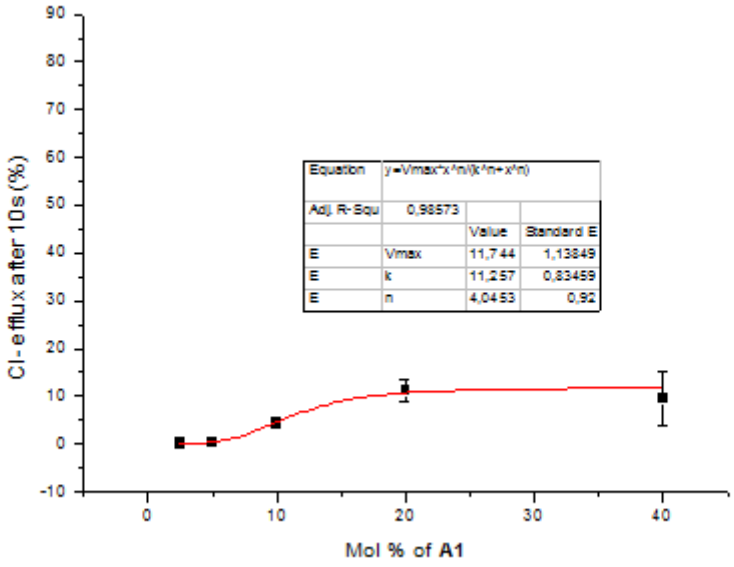

Supplementary figure S19. Hill plot for chloride release mediated by compound **1** from EYPC LUVs loaded with 100 mM NaCl buffered to pH 6.4 with 10 mM phosphate buffer. The vesicles were dispersed in 100 mM $NaNO_3$ buffered to pH 6.4 with 10 mM phosphate buffer. Chloride efflux was measured 10 s after injection.

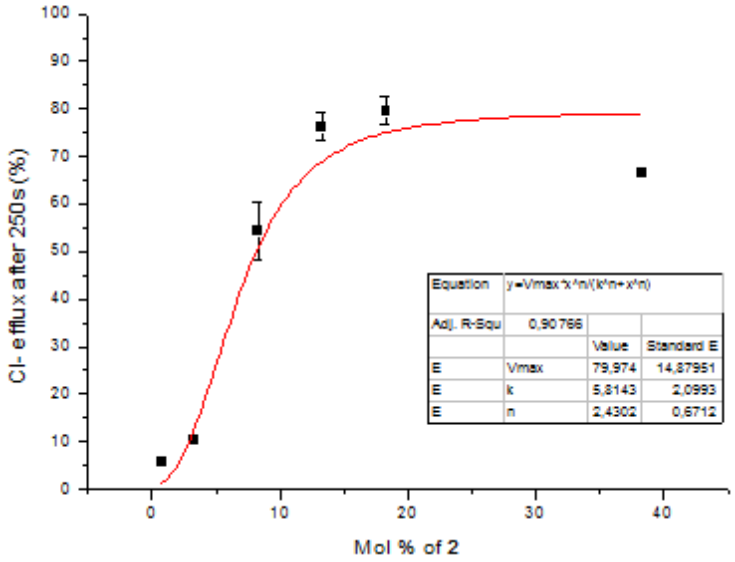

Supplementary figure S20. Hill plot for chloride release mediated by compound **2** from EYPC LUVs loaded with 100 mM NaCl buffered to pH 6.4 with 10 mM phosphate buffer. The vesicles were dispersed in 100 mM $NaNO_3$ buffered to pH 6.4 with 10 mM phosphate buffer. Chloride efflux was measured 10 s after injection.

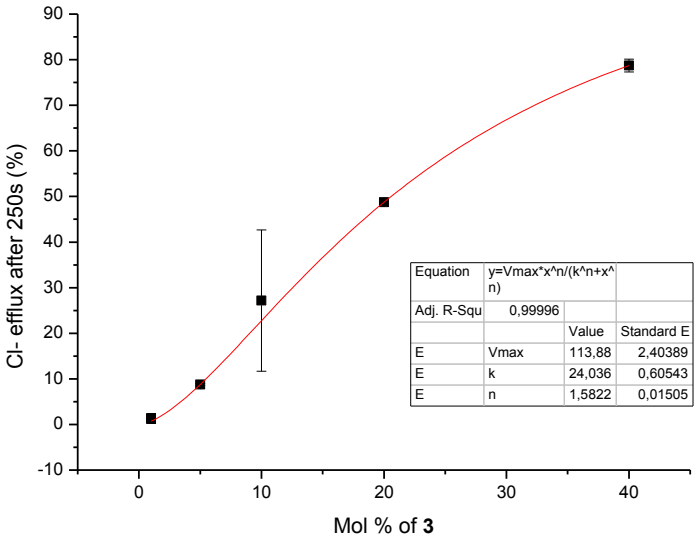

Supplementary figure S21. Hill plot for chloride release mediated by compound **3** from EYPC LUVs loaded with 100 mM NaCl buffered to pH 6.4 with 10 mM phosphate buffer. The vesicles were dispersed in 100 mM $NaNO_3$ buffered to pH 6.4 with 10 mM phosphate buffer. Chloride efflux was measured 250 s after injection.

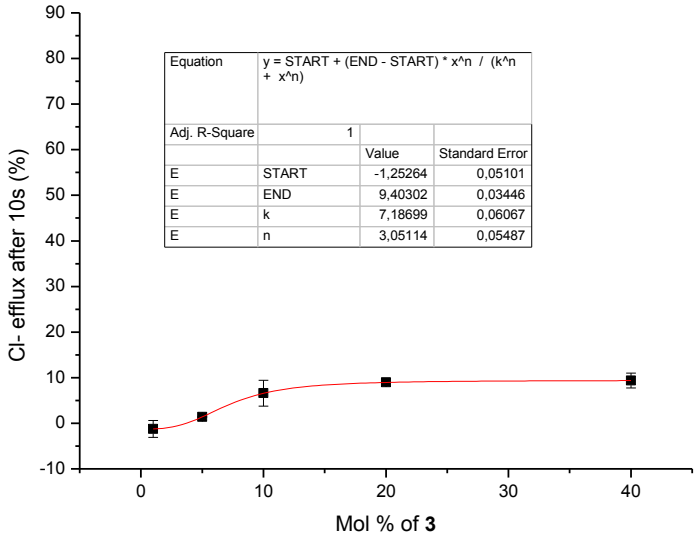

Supplementary figure S22. Hill plot for chloride release mediated by compound **3** from EYPC LUVs loaded with 100 mM NaCl buffered to pH 6.4 with 10 mM phosphate buffer. The vesicles were dispersed in 100 mM $NaNO_3$ buffered to pH 6.4 with 10 mM phosphate buffer. Chloride efflux was measured 10 s after injection.

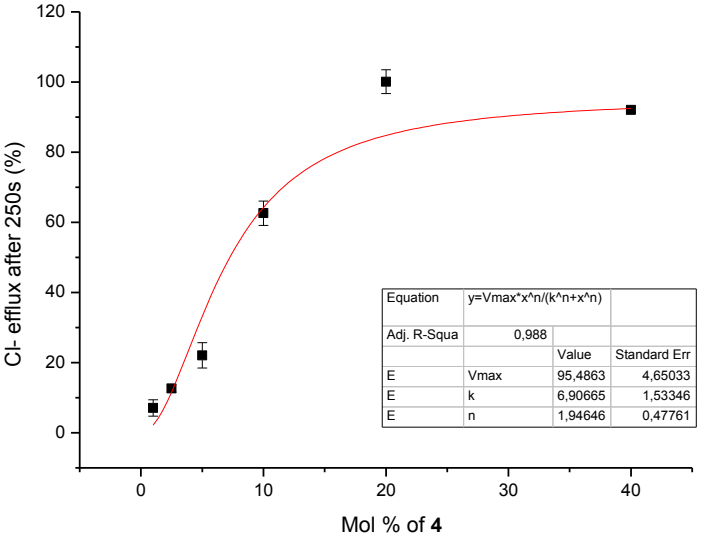

Supplementary figure S23. Hill plot for chloride release mediated by compound **4** from EYPC LUVs loaded with 100 mM NaCl buffered to pH 6.4 with 10 mM phosphate buffer. The vesicles were dispersed in 100 mM $NaNO_3$ buffered to pH 6.4 with 10 mM phosphate buffer. Chloride efflux was measured 250 s after injection.

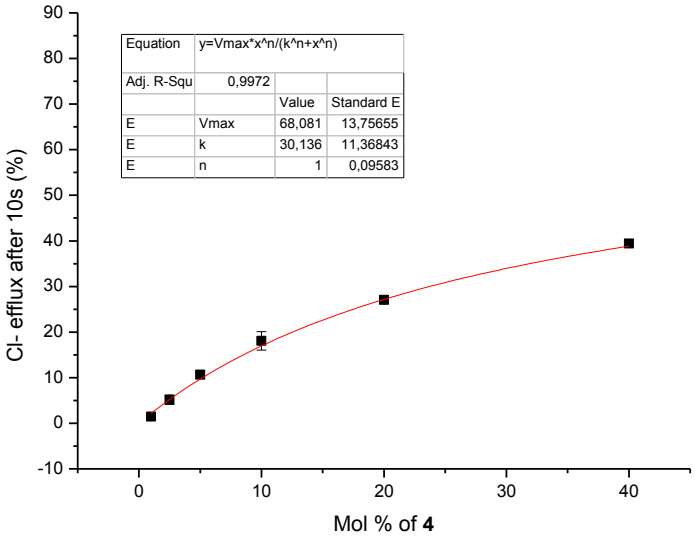

Supplementary figure S24. Hill plot for chloride release mediated by compound **4** from EYPC LUVs loaded with 100 mM NaCl buffered to pH 6.4 with 10 mM phosphate buffer. The vesicles were dispersed in 100 mM $NaNO_3$ buffered to pH 6.4 with 10 mM phosphate buffer. Chloride efflux was measured 10 s after injection.

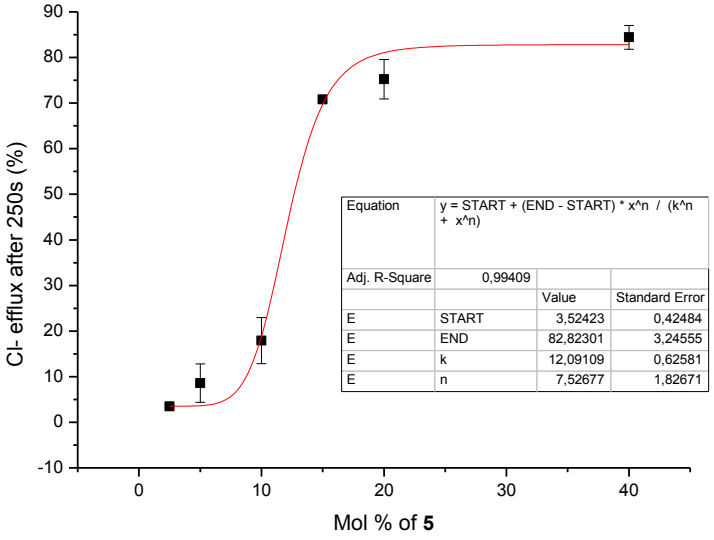

Supplementary figure S25. Hill plot for chloride release mediated by compound **5** from EYPC LUVs loaded with 100 mM NaCl buffered to pH 6.4 with 10 mM phosphate buffer. The vesicles were dispersed in 100 mM $NaNO_3$ buffered to pH 6.4 with 10 mM phosphate buffer. Chloride efflux was measured 250 s after injection.

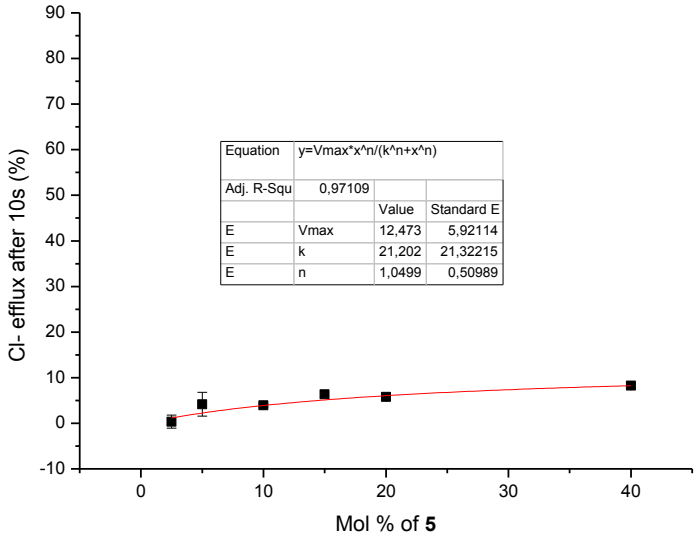

Supplementary figure S26. Hill plot for chloride release mediated by compound **5** from EYPC LUVs loaded with 100 mM NaCl buffered to pH 6.4 with 10 mM phosphate buffer. The vesicles were dispersed in 100 mM $NaNO_3$ buffered to pH 6.4 with 10 mM phosphate buffer. Chloride efflux was measured 10 s after injection.

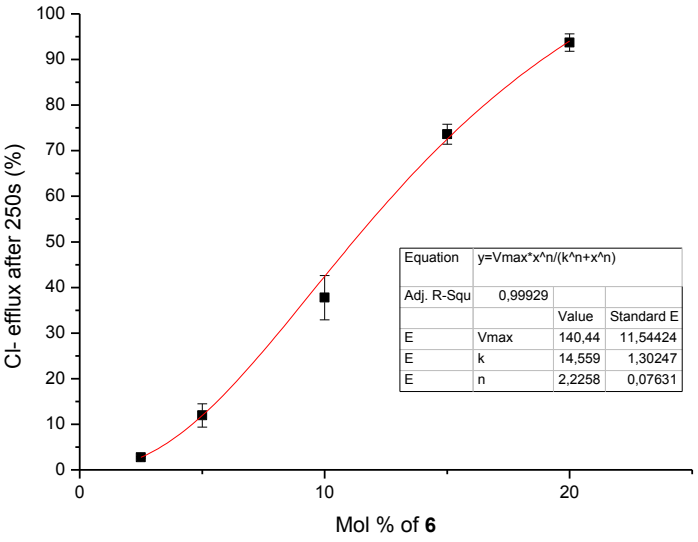

Supplementary figure S27. Hill plot for chloride release mediated by compound **6** from EYPC LUVs loaded with 100 mM NaCl buffered to pH 6.4 with 10 mM phosphate buffer. The vesicles were dispersed in 100 mM $NaNO_3$ buffered to pH 6.4 with 10 mM phosphate buffer. Chloride efflux was measured 250 s after injection.

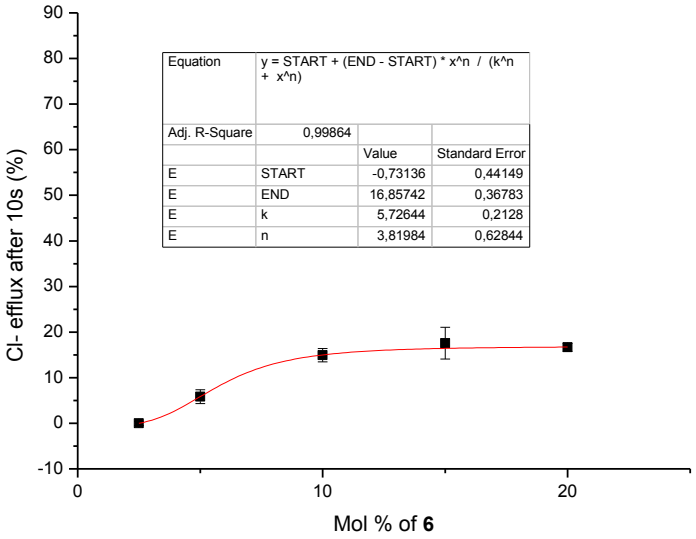

Supplementary figure S28. Hill plot for chloride release mediated by compound **6** from EYPC LUVs loaded with 100 mM NaCl buffered to pH 6.4 with 10 mM phosphate buffer. The vesicles were dispersed in 100 mM $NaNO_3$ buffered to pH 6.4 with 10 mM phosphate buffer. Chloride efflux was measured 10 s after injection.

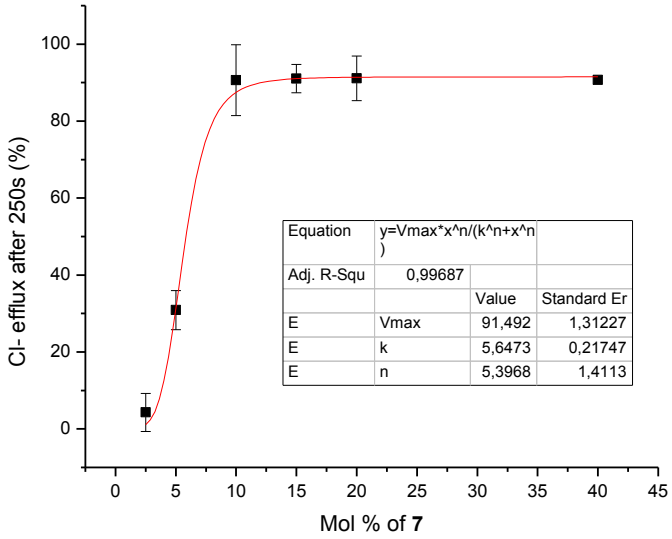

Supplementary figure S29. Hill plot for chloride release mediated by compound **7** from EYPC LUVs loaded with 100 mM NaCl buffered to pH 6.4 with 10 mM phosphate buffer. The vesicles were dispersed in 100 mM $NaNO_3$ buffered to pH 6.4 with 10 mM phosphate buffer. Chloride efflux was measured 250 s after injection.

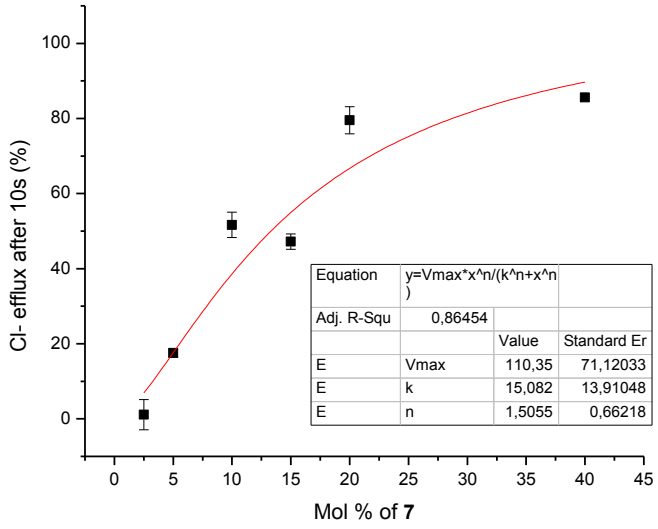

Supplementary figure S30. Hill plot for chloride release mediated by compound **7** from EYPC LUVs loaded with 100 mM NaCl buffered to pH 6.4 with 10 mM phosphate buffer. The vesicles were dispersed in 100 mM $NaNO_3$ buffered to pH 6.4 with 10 mM phosphate buffer. Chloride efflux was measured 250 s after injection.

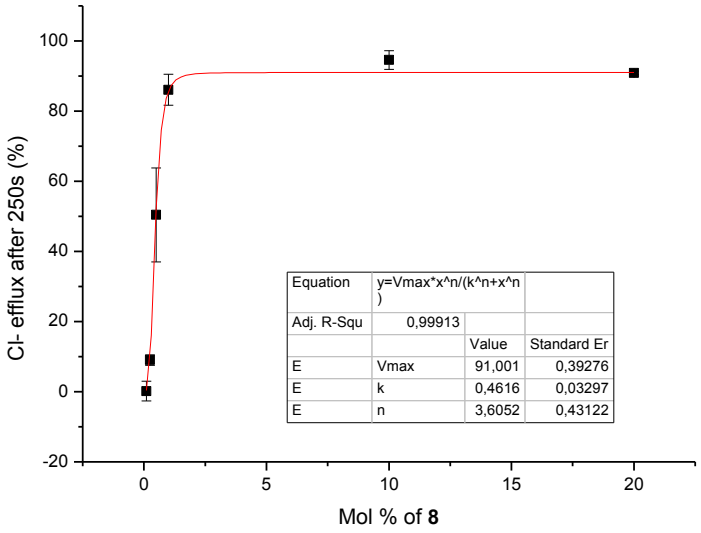

Supplementary figure S31. Hill plot for chloride release mediated by compound **8** from EYPC LUVs loaded with 100 mM NaCl buffered to pH 6.4 with 10 mM phosphate buffer. The vesicles were dispersed in 100 mM $NaNO_3$ buffered to pH 6.4 with 10 mM phosphate buffer. Chloride efflux was measured 250 s after injection.

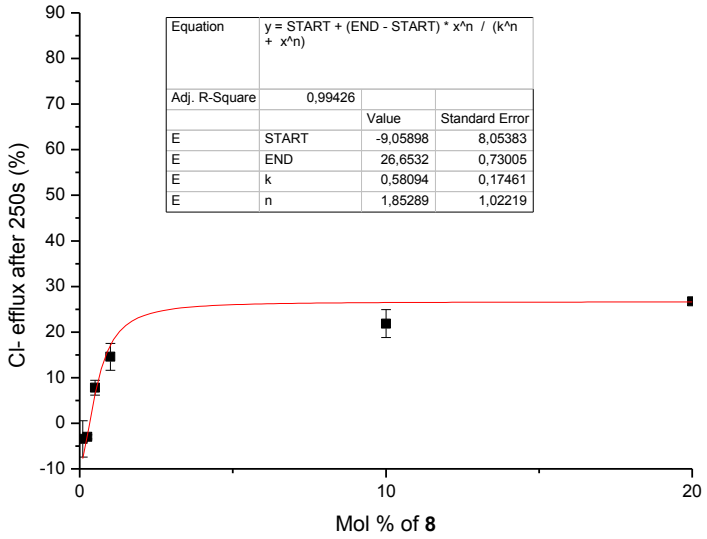

Supplementary figure S32. Hill plot for chloride release mediated by compound **8** from EYPC LUVs loaded with 100 mM NaCl buffered to pH 6.4 with 10 mM phosphate buffer. The vesicles were dispersed in 100 mM $NaNO_3$ buffered to pH 6.4 with 10 mM phosphate buffer. Chloride efflux was measured 10 s after injection.

U-tube experiment

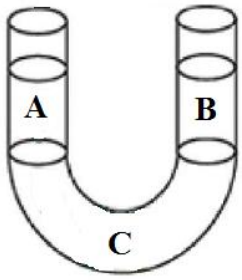

Supplementary figure S33. U-tube experiment scheme. A: Aqueous donating phase containing 0.1 mM Lucigenin (water, 5 mL). B: Receiving phase (water, 5 mL). C: Bulk organic phase ($CHCl_3$, 10 mL) with ionophore (1mM) or without.

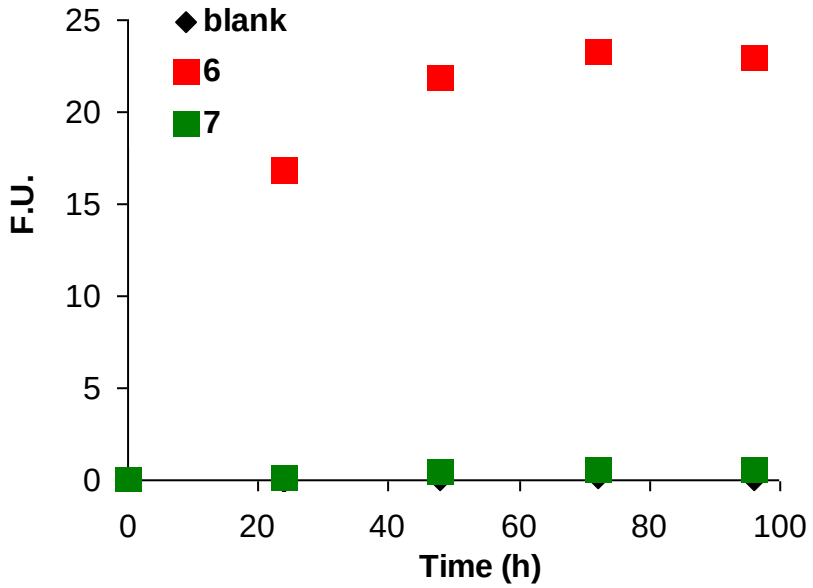

Supplementary figure S34. Increase of the lucigenin's fluorescence in U-tube tests in the presence of compounds **6**,**7** and the blank.

Minimal inhibitory concentration (MIC) determination

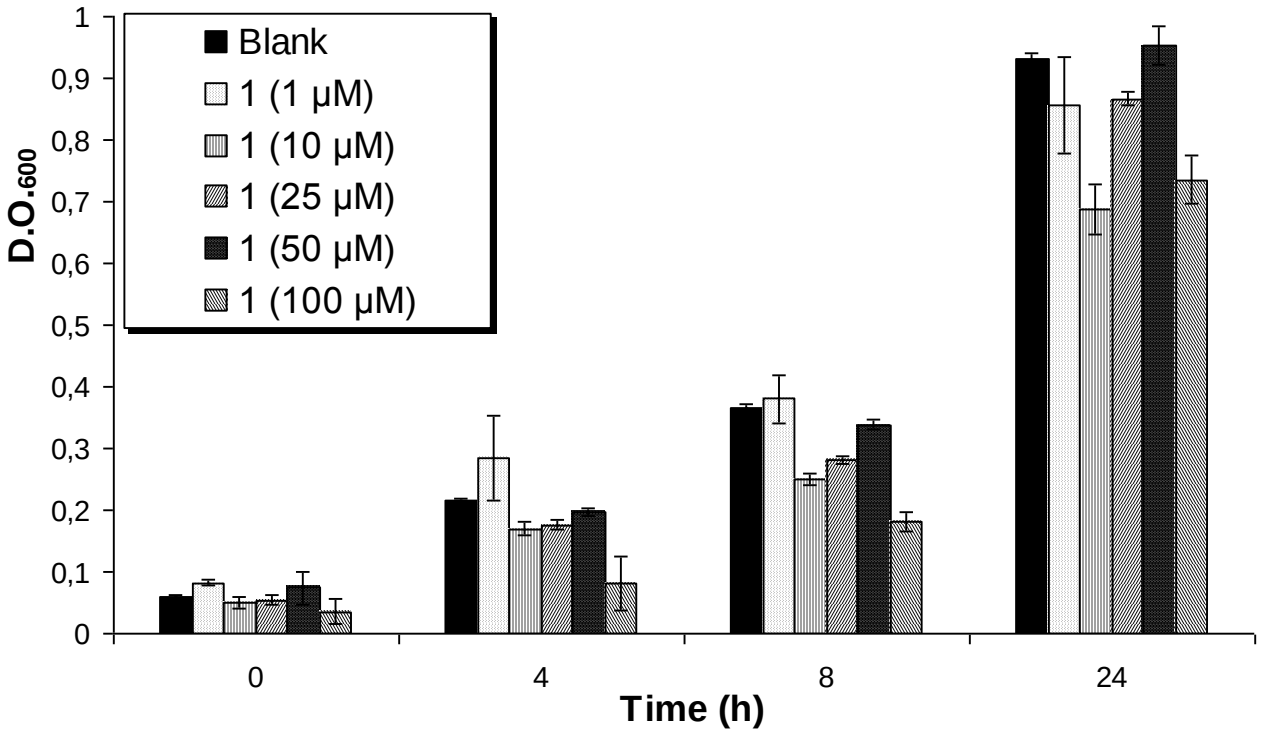

Supplementary figure S35. Dose-dependent growth inhibition of *E.coli (DH5α)* by **1**.

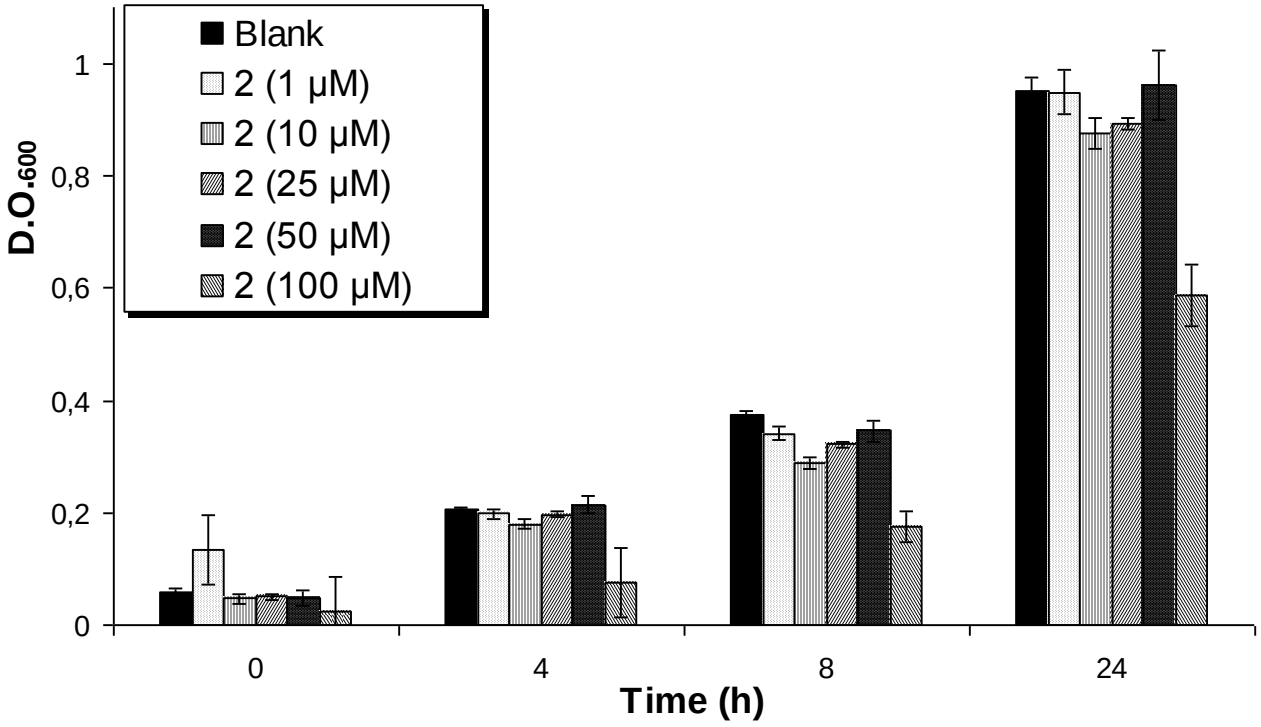

Supplementary figure S36. Dose-dependent growth inhibition of *E.coli (DH5α)* by **2**.

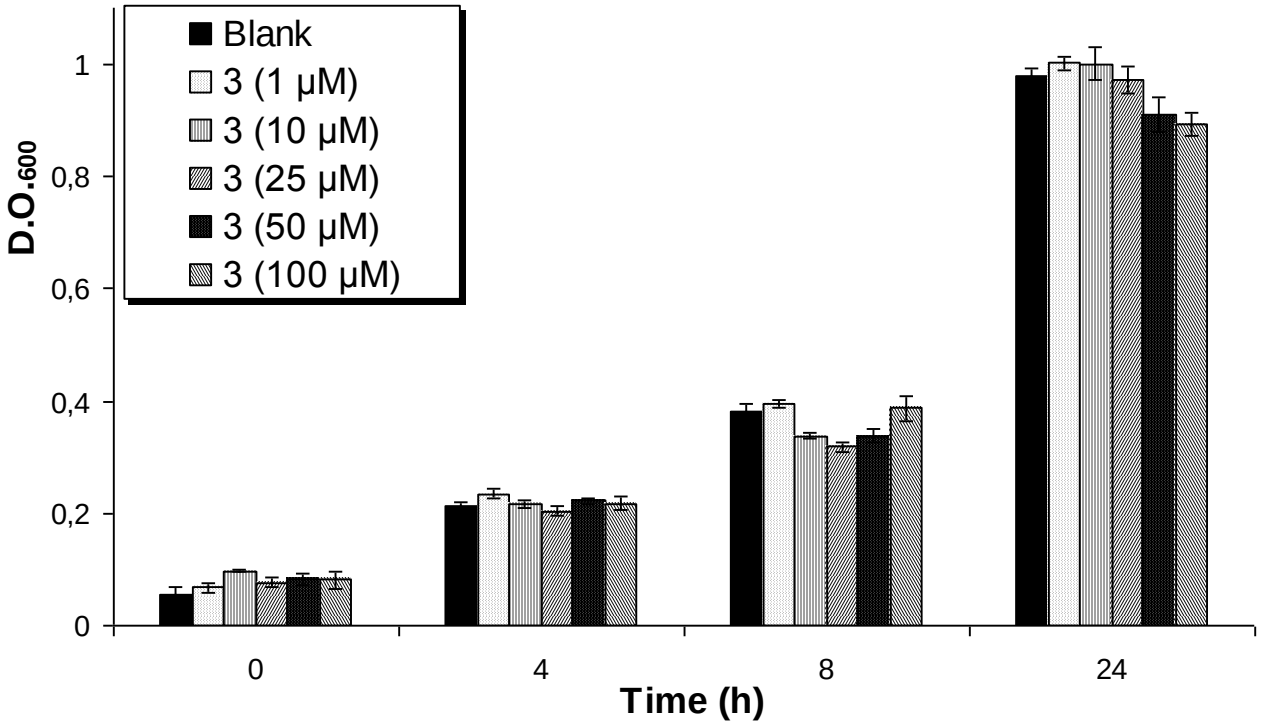

Supplementary figure S37. Dose-dependent growth inhibition of *E.coli (DH5α)* by **3**.

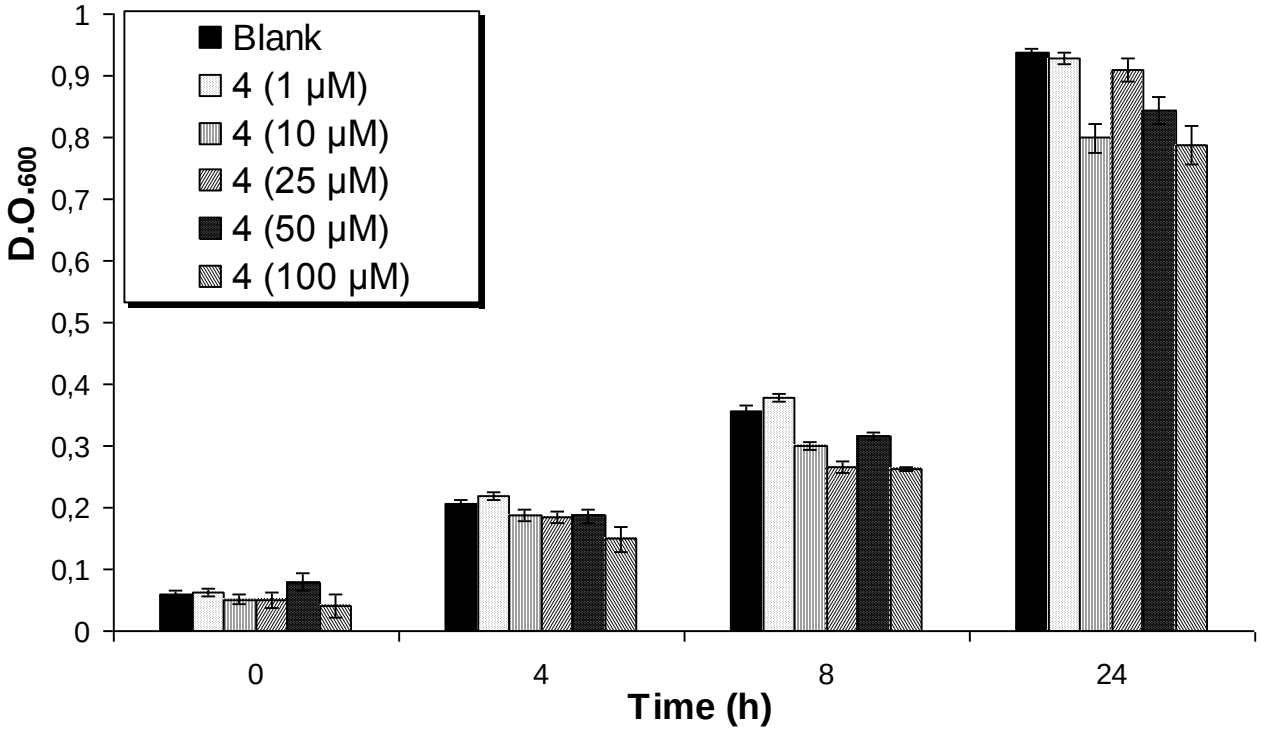

Supplementary figure S38. Dose-dependent growth inhibition of *E.coli (DH5α)* by **4**.

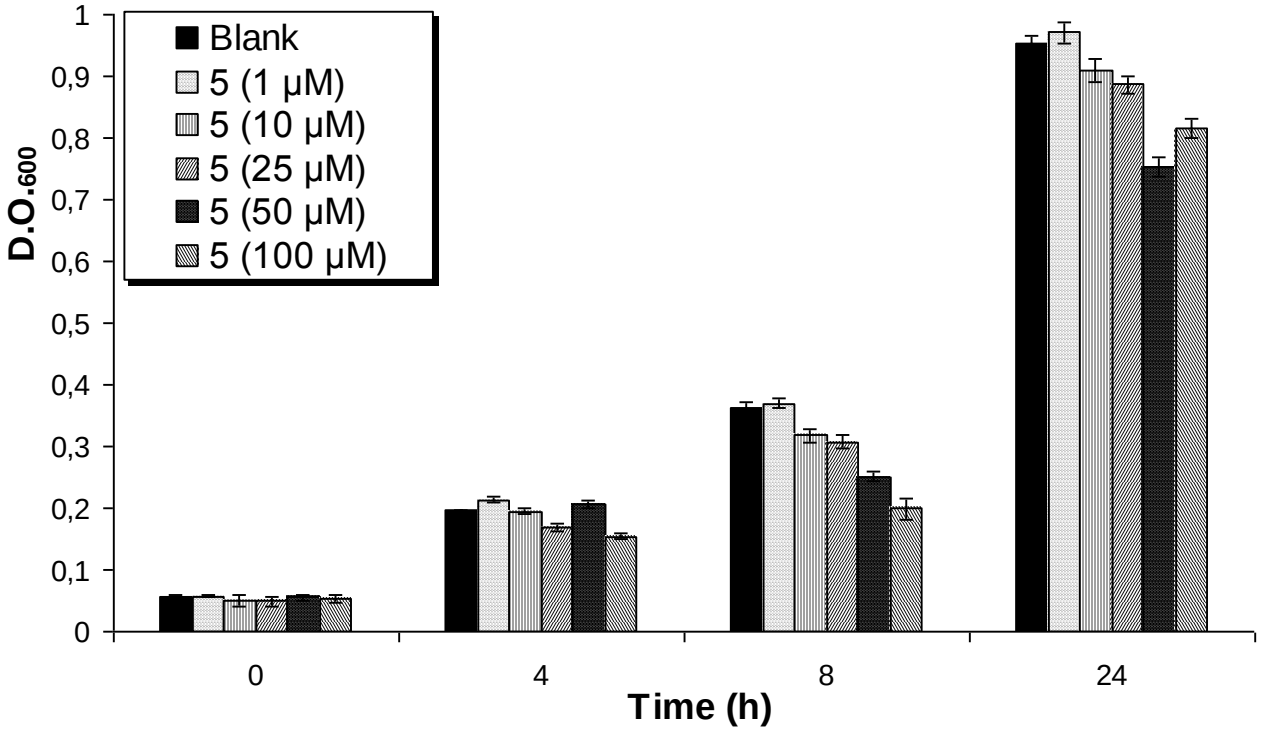

Supplementary figure S39. Dose-dependent growth inhibition of *E.coli (DH5α)* by **5**.

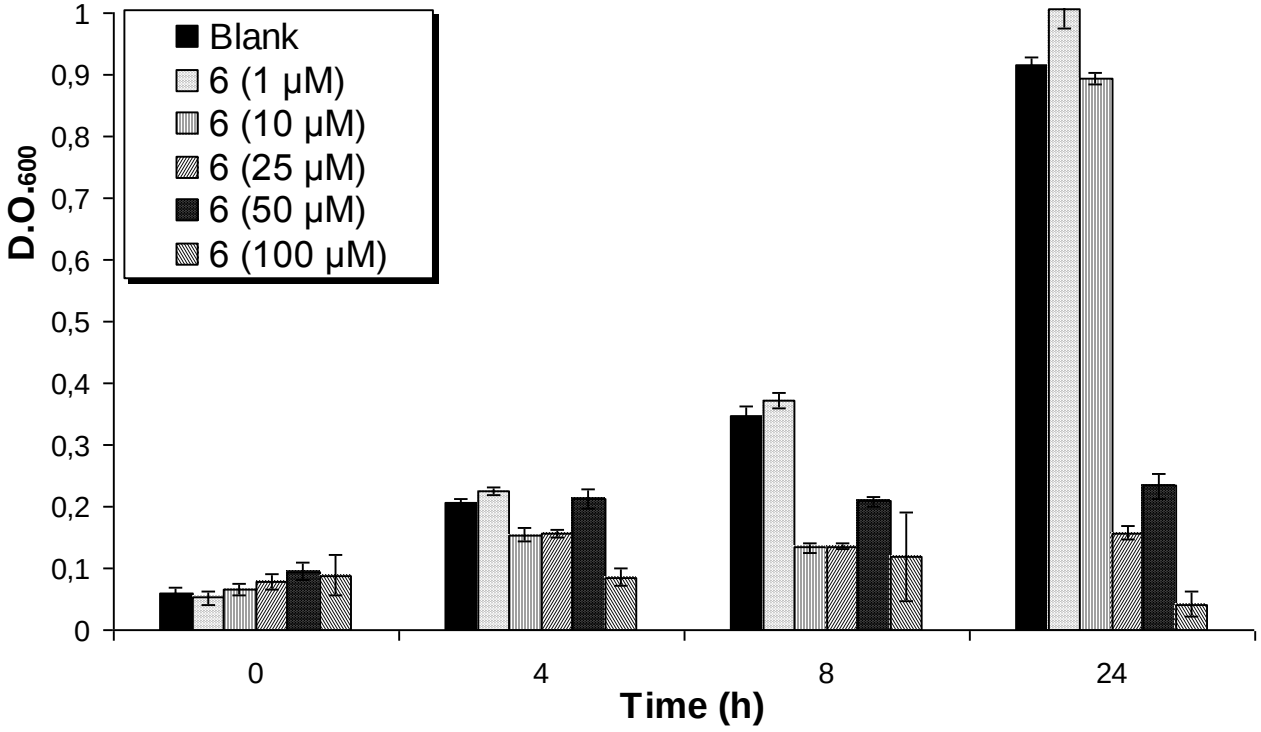

Supplementary figure S40. Dose-dependent growth inhibition of *E.coli (DH5α)* by **6**.

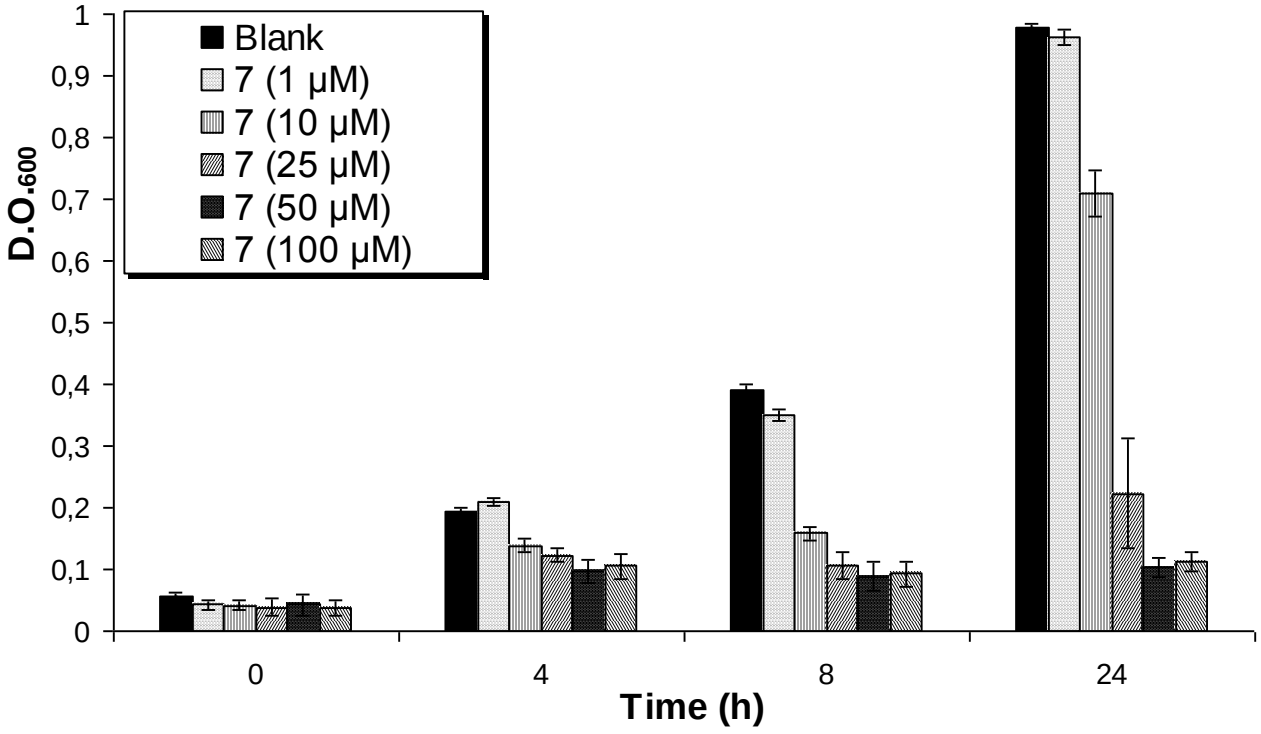

Supplementary figure S41. Dose-dependent growth inhibition of *E.coli (DH5α)* by **7**.

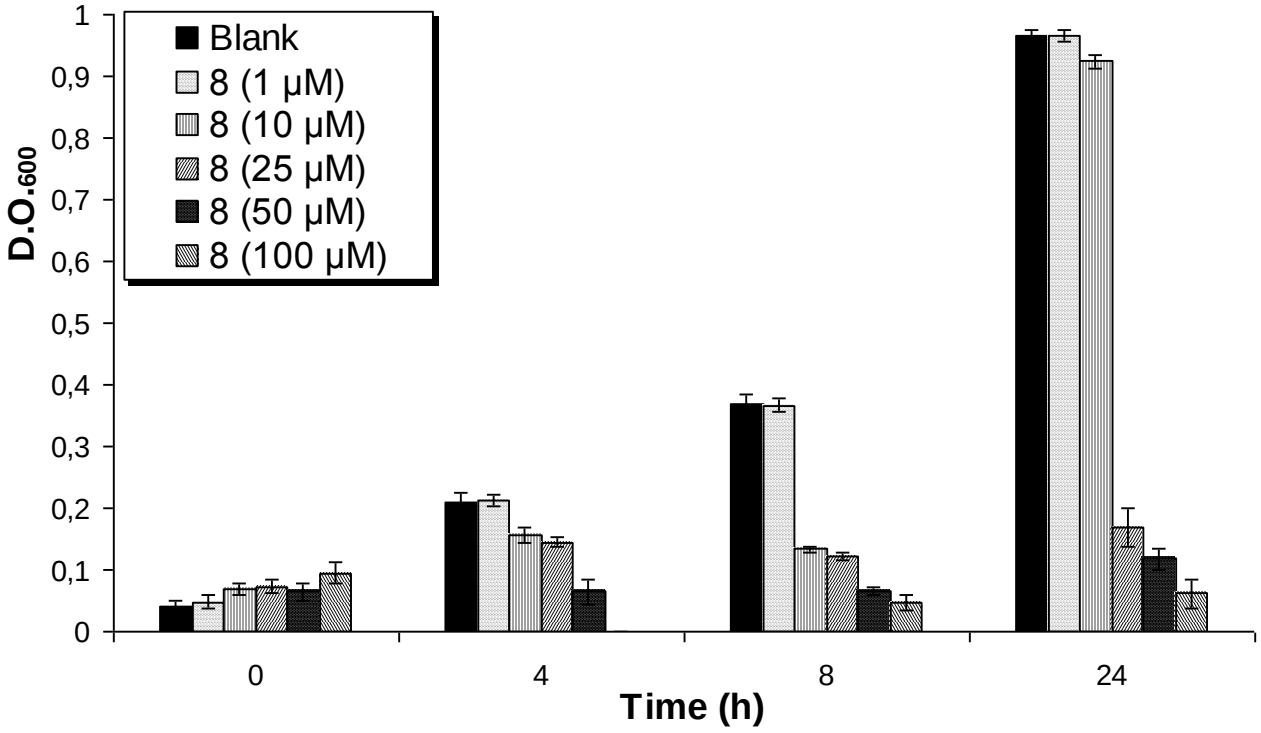

Supplementary figure S42. Dose-dependent growth inhibition of *E.coli (DH5α)* by **8**.

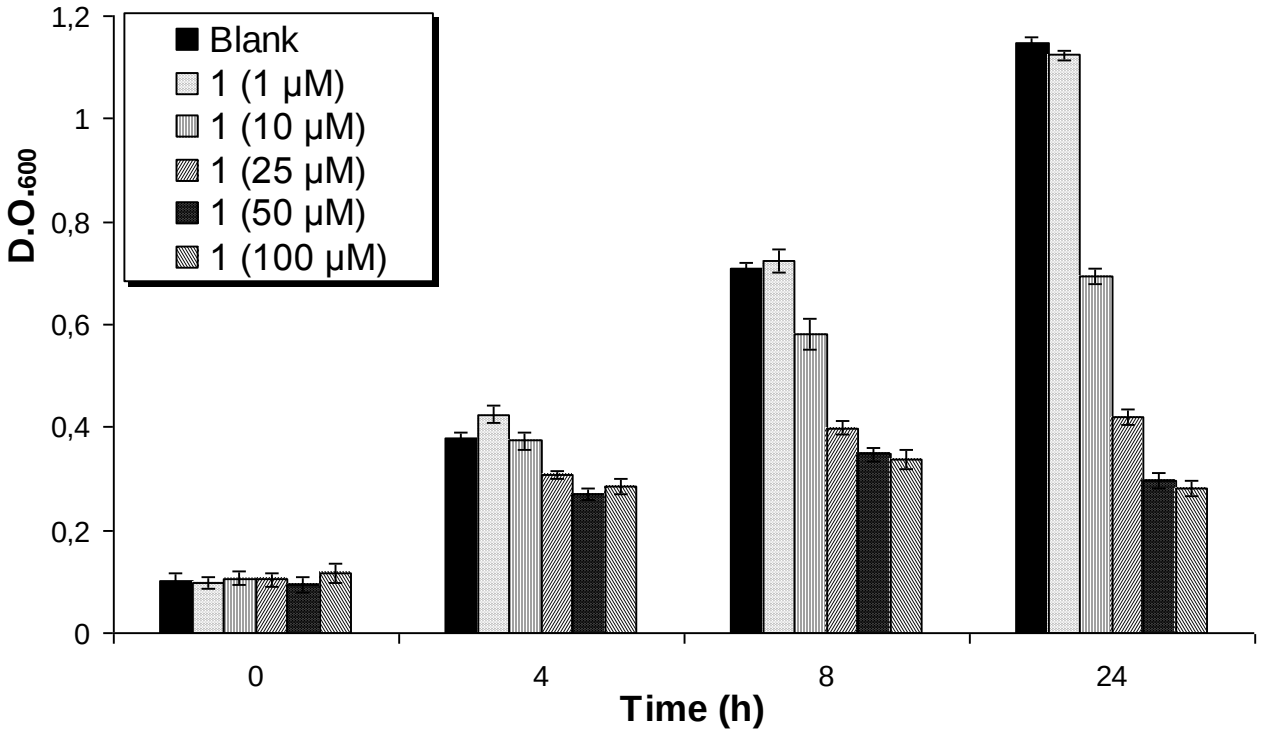

Supplementary figure S43. Dose-dependent growth inhibition of *E.coli (SK037)* by **1**.

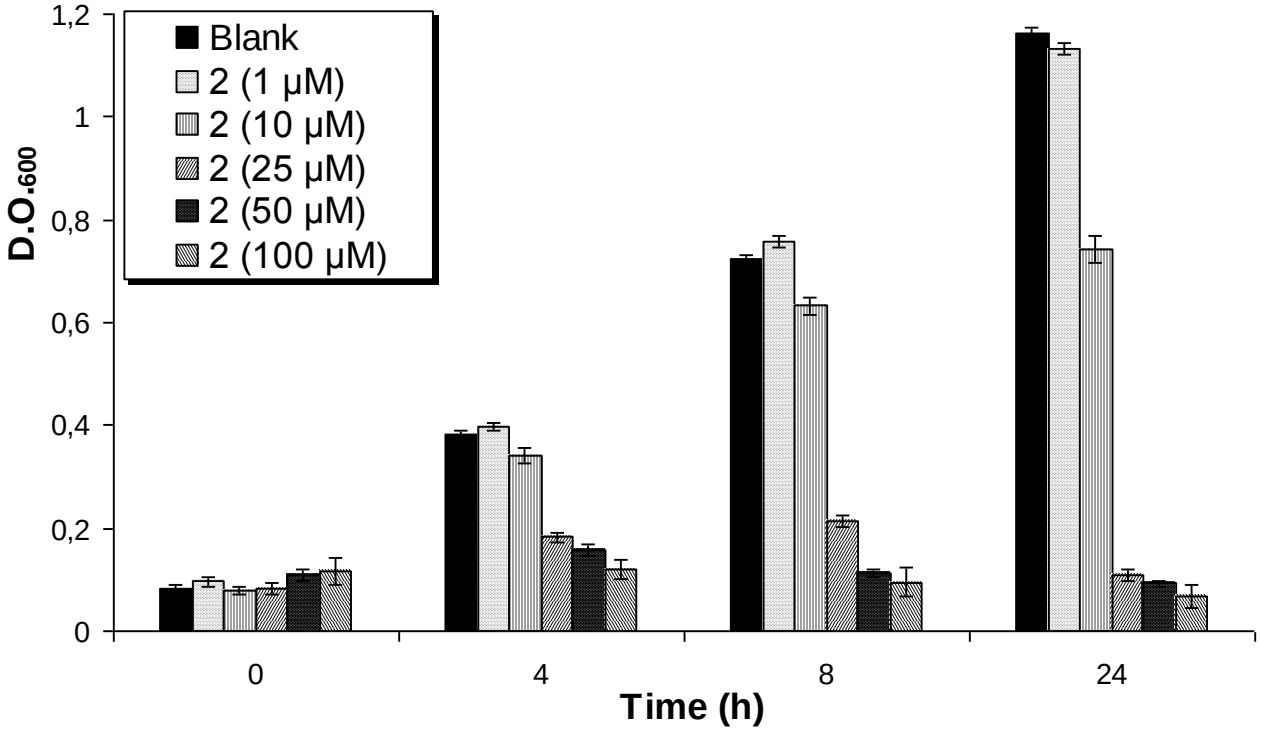

Supplementary figure S44. Dose-dependent growth inhibition of *E.coli (SK037)* by **2**.

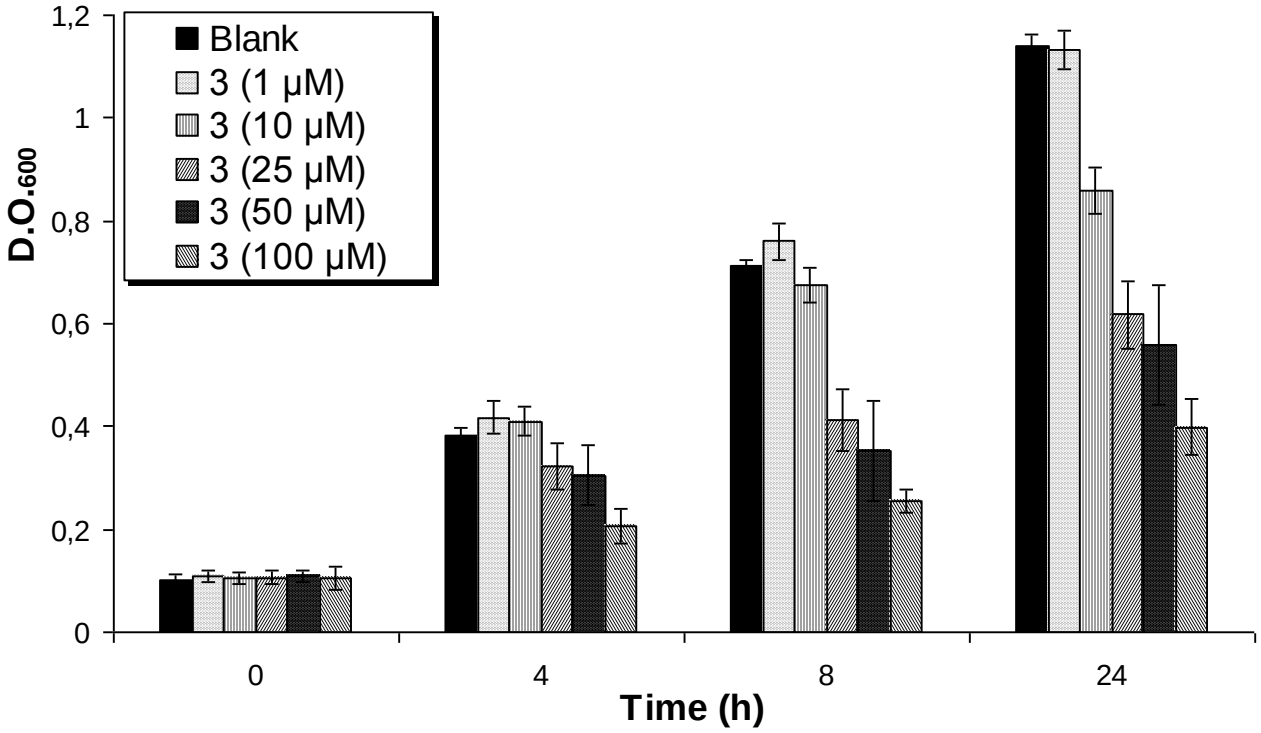

Supplementary figure S45. Dose-dependent growth inhibition of *E.coli (SK037)* by **3**.

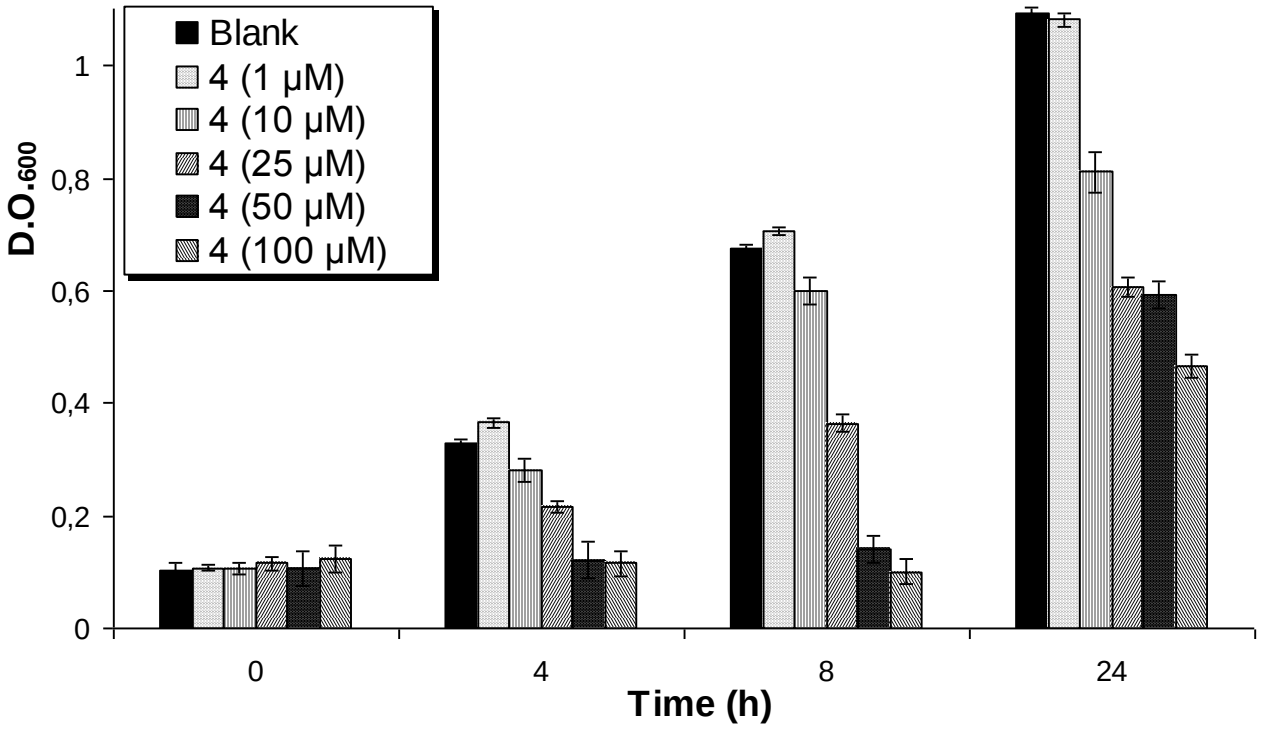

Supplementary figure S46. Dose-dependent growth inhibition of *E.coli (SK037)* by **4**.

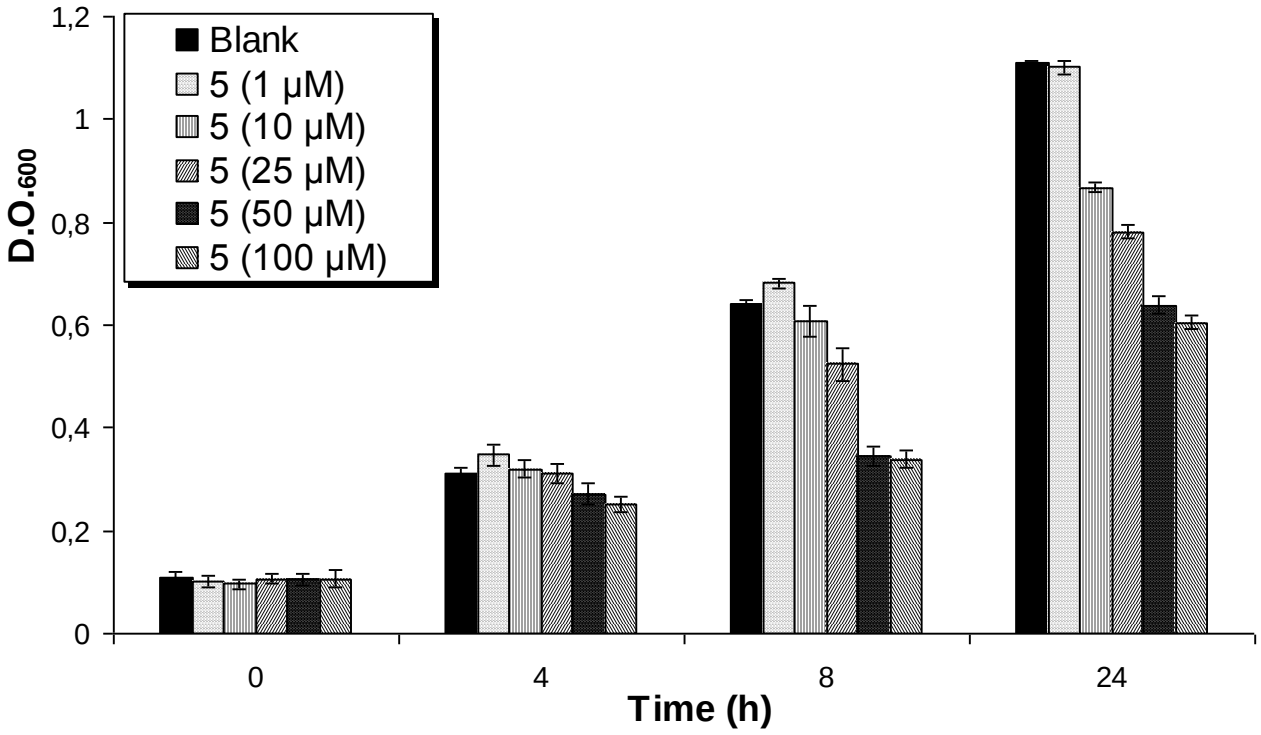

Supplementary figure S47. Dose-dependent growth inhibition of *E.coli (SK037)* by **5**.

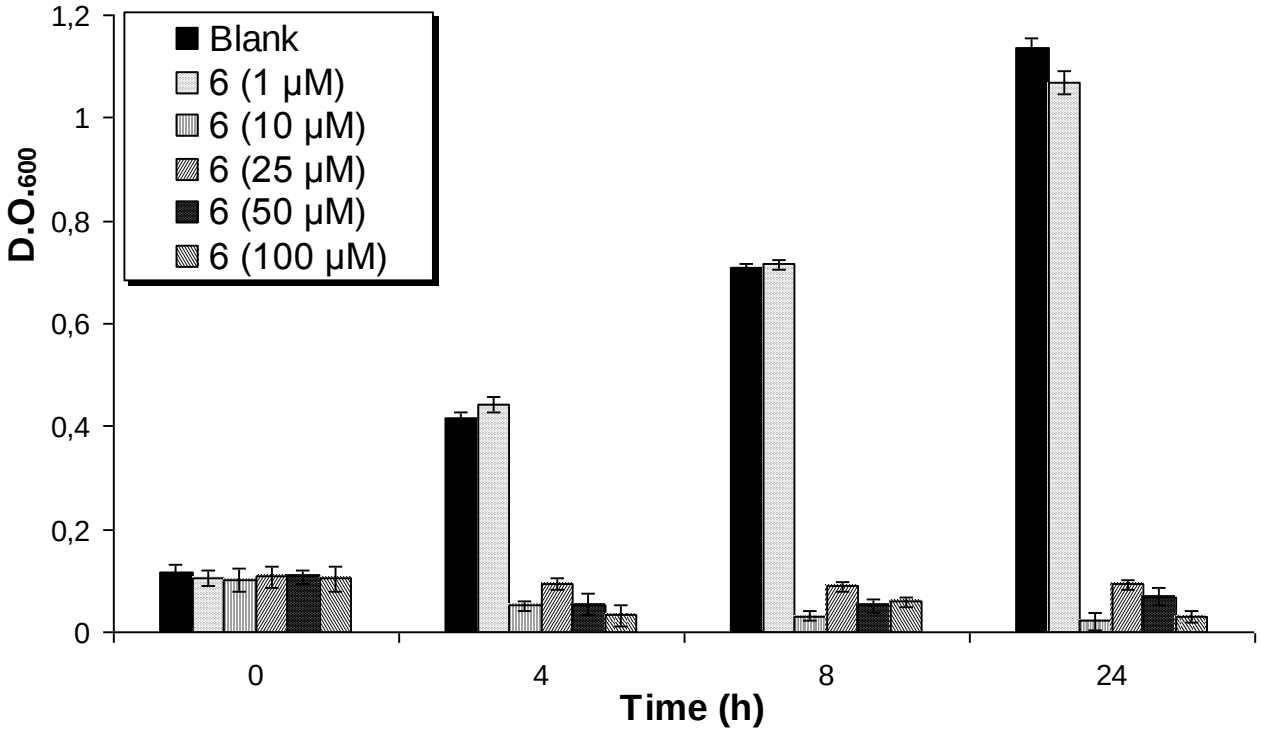

Supplementary figure S48. Dose-dependent growth inhibition of *E.coli (SK037)* by **6**.

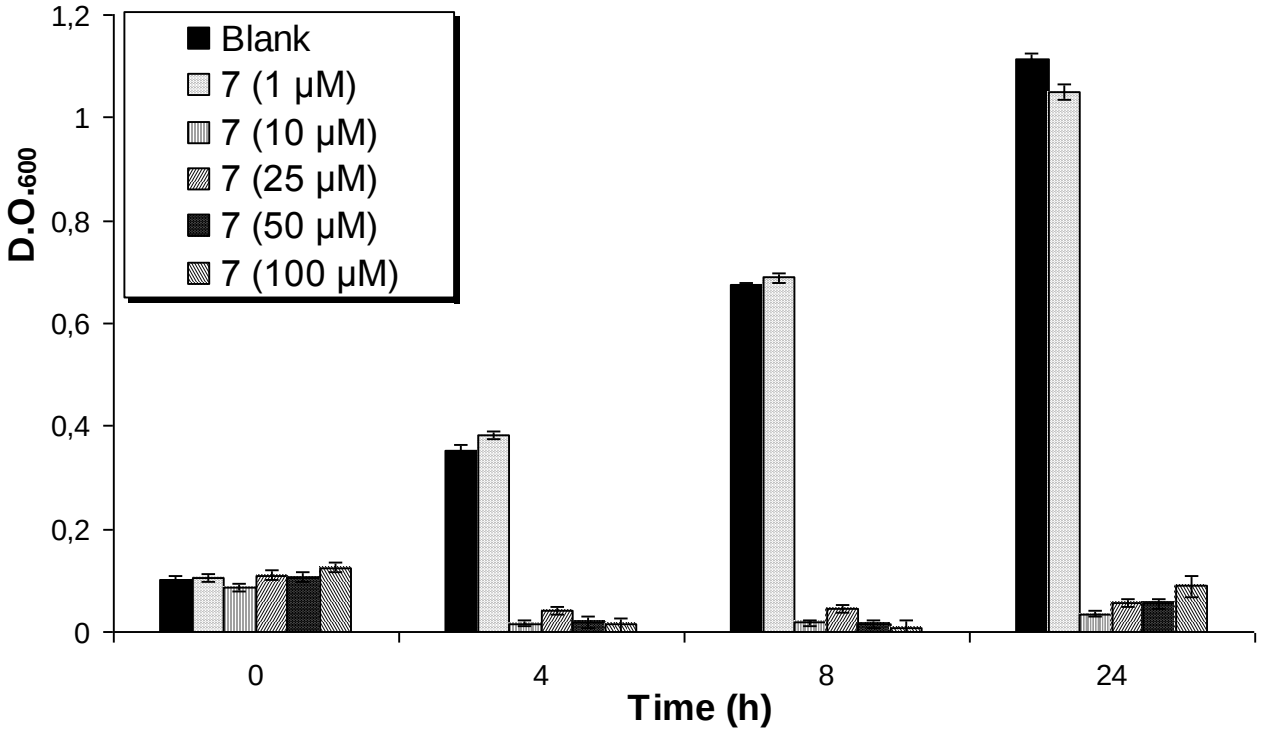

Supplementary figure S49. Dose-dependent growth inhibition of *E.coli (SK037)* by **7**.

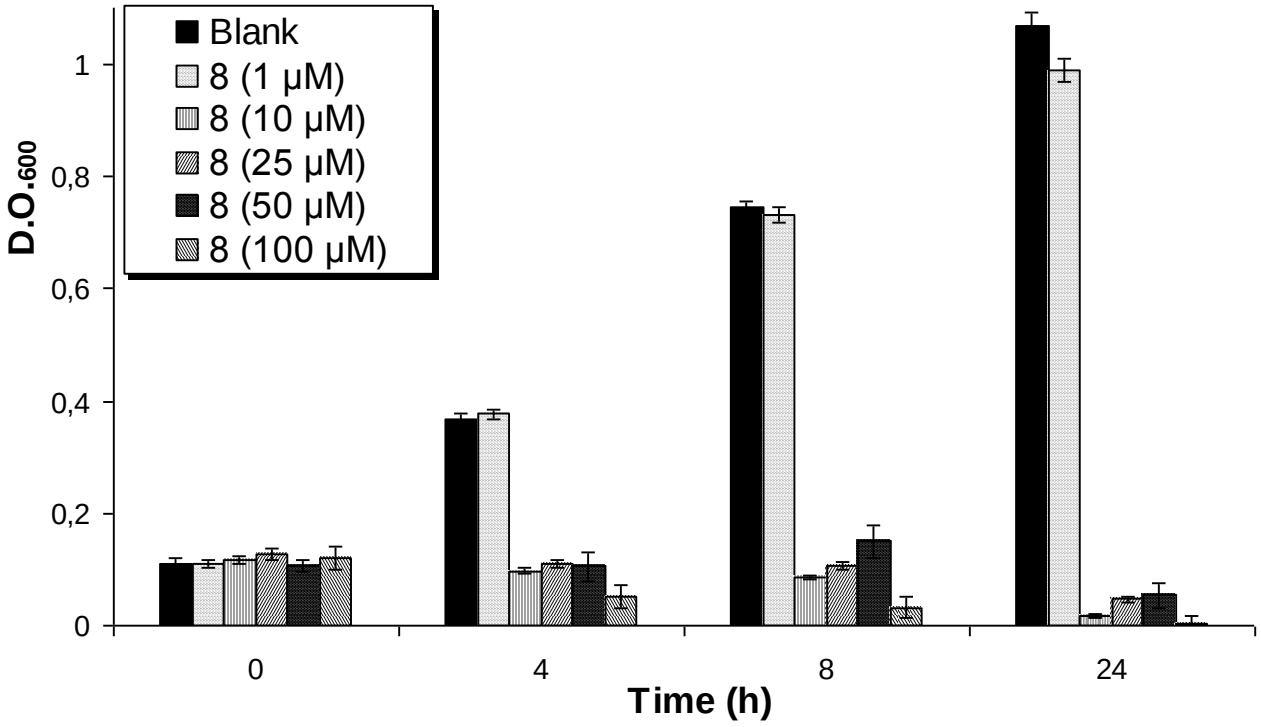

Supplementary figure S50. Dose-dependent growth inhibition of *E.coli (SK037)* by **8**.

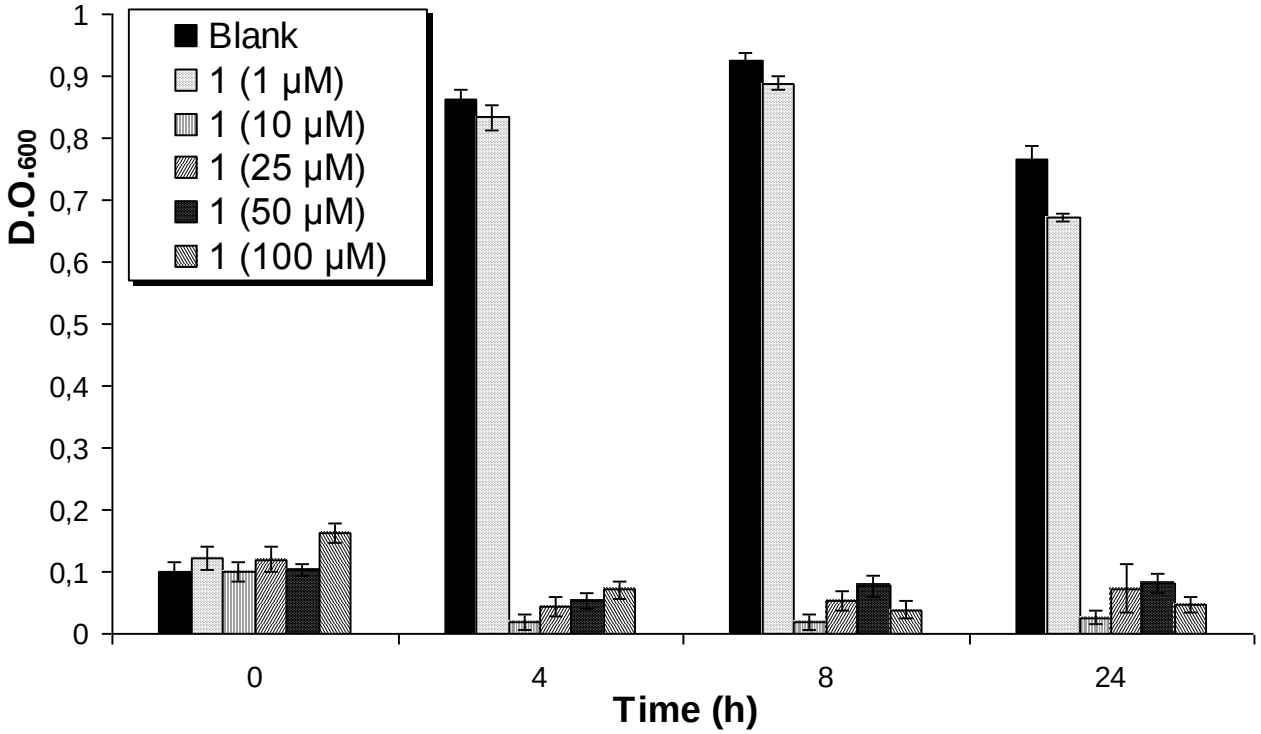

Supplementary figure S51. Dose-dependent growth inhibition of *B.thuringiensis (HD73)* by **1**.

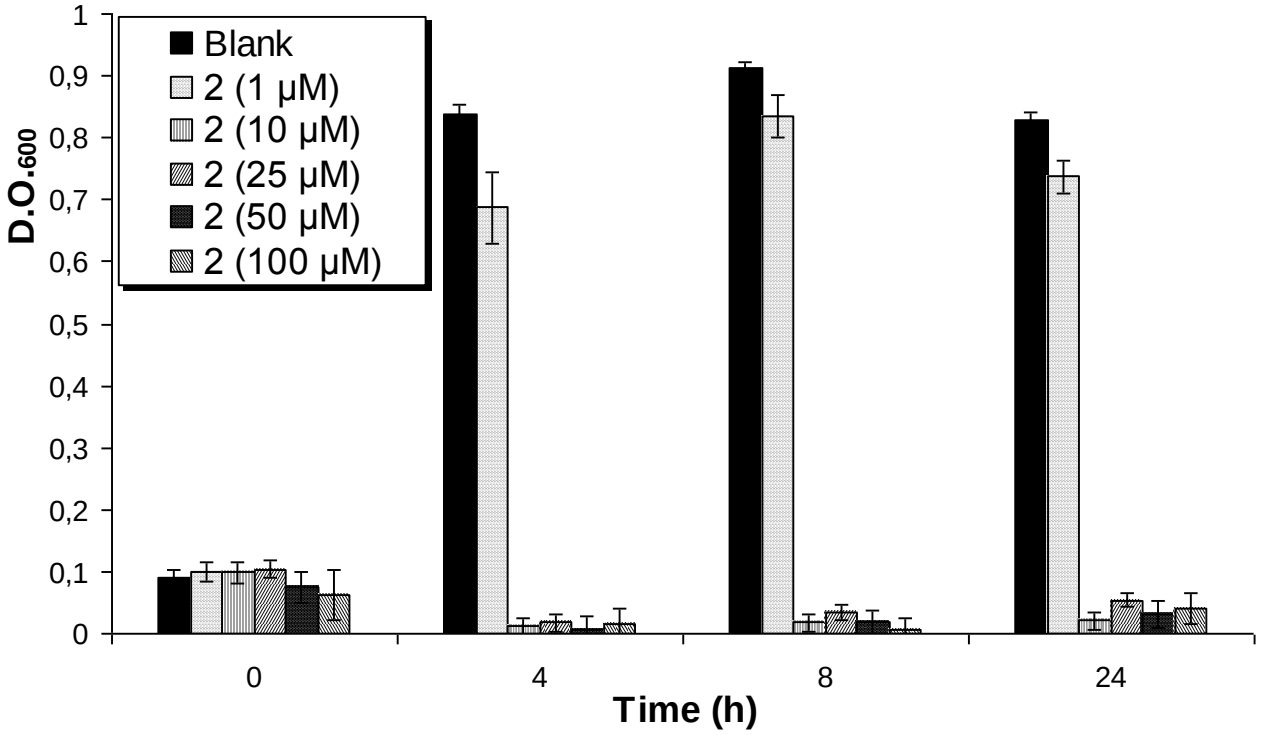

Supplementary figure S52. Dose-dependent growth inhibition of *B.thuringiensis (HD73)* by **2**.

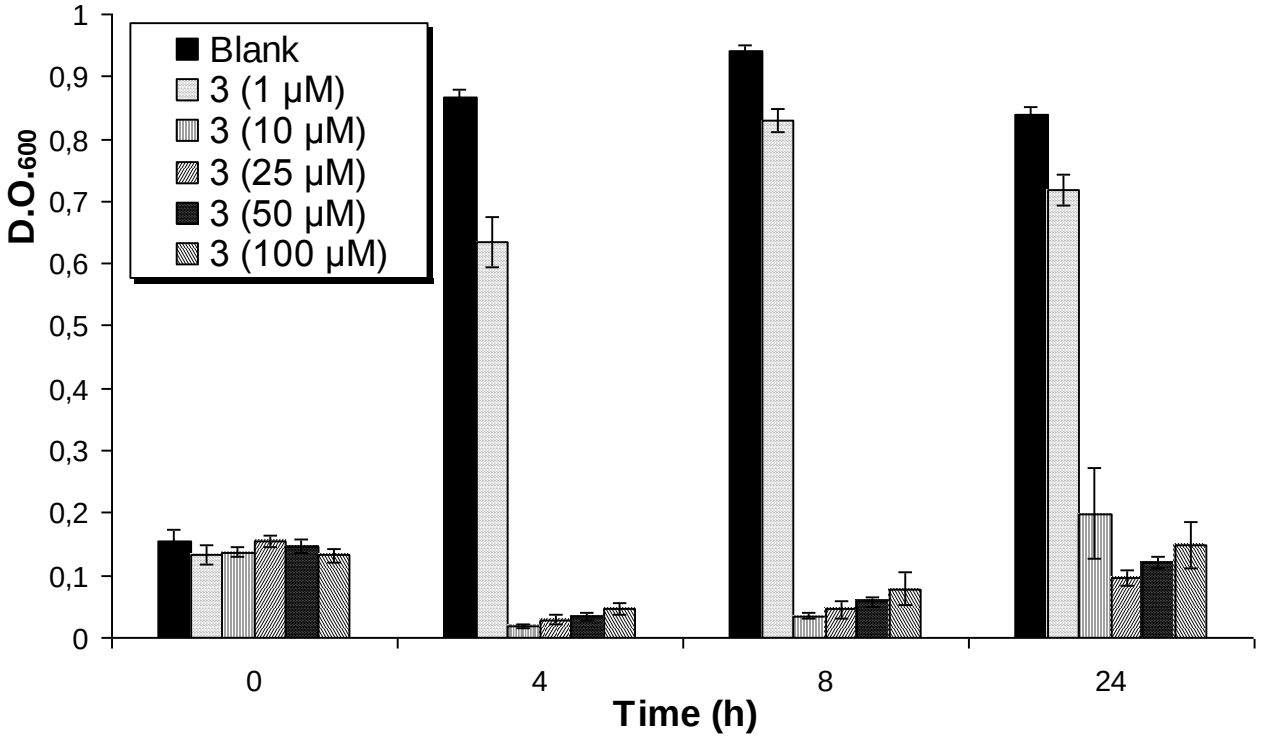

Supplementary figure S53. Dose-dependent growth inhibition of *B.thuringiensis (HD73)* by **3**.

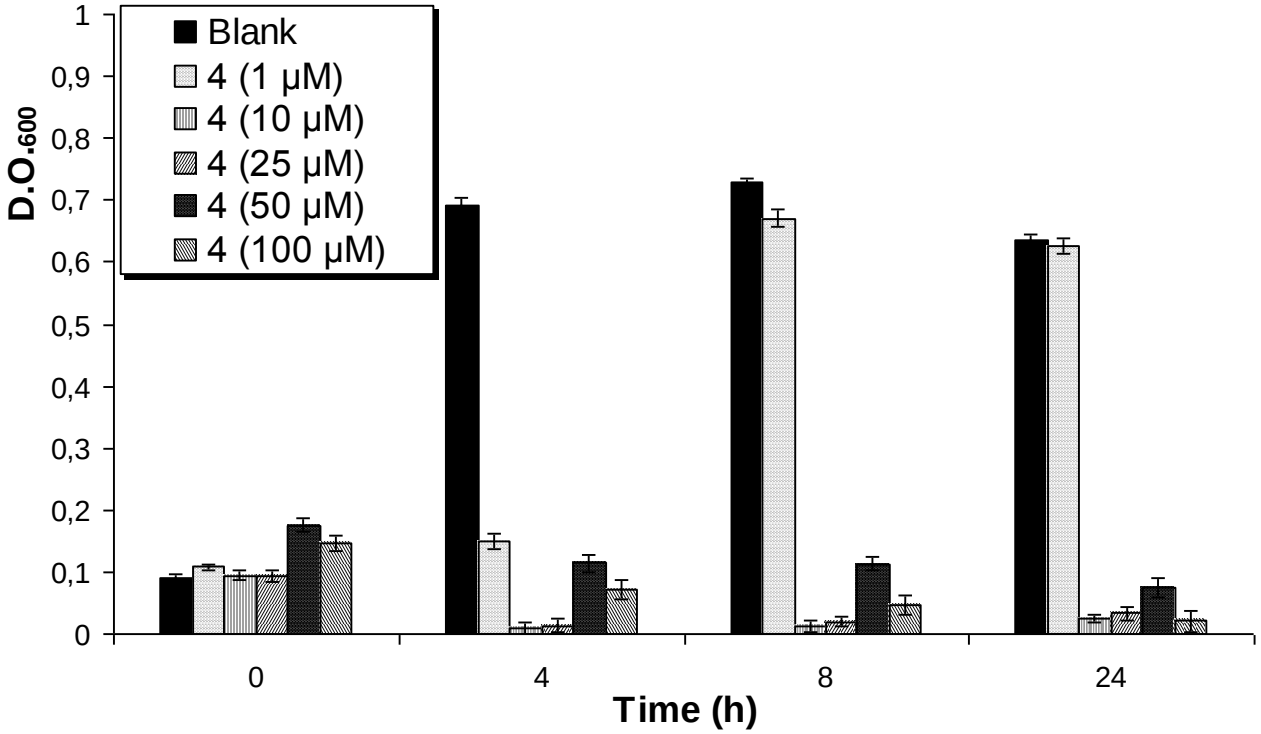

Supplementary figure S54. Dose-dependent growth inhibition of *B.thuringiensis (HD73)* by **4**.

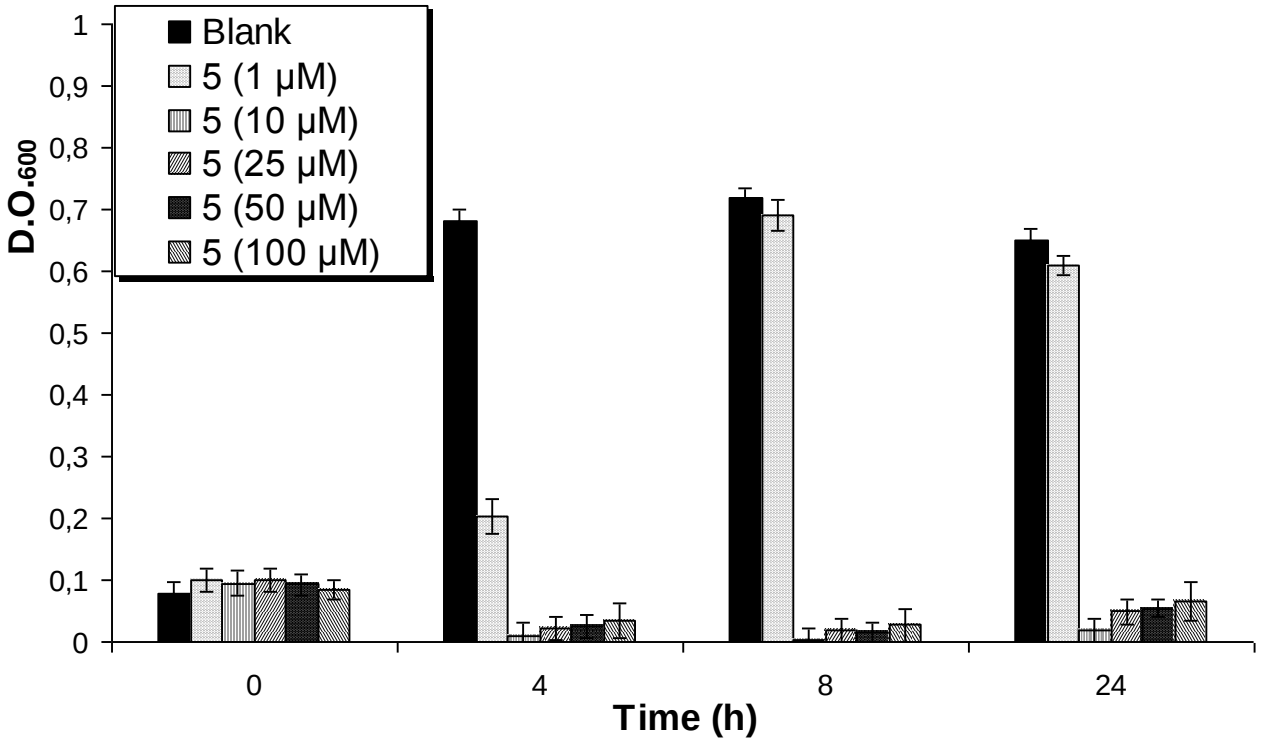

Supplementary figure S55. Dose-dependent growth inhibition of *B.thuringiensis (HD73)* by **5**.

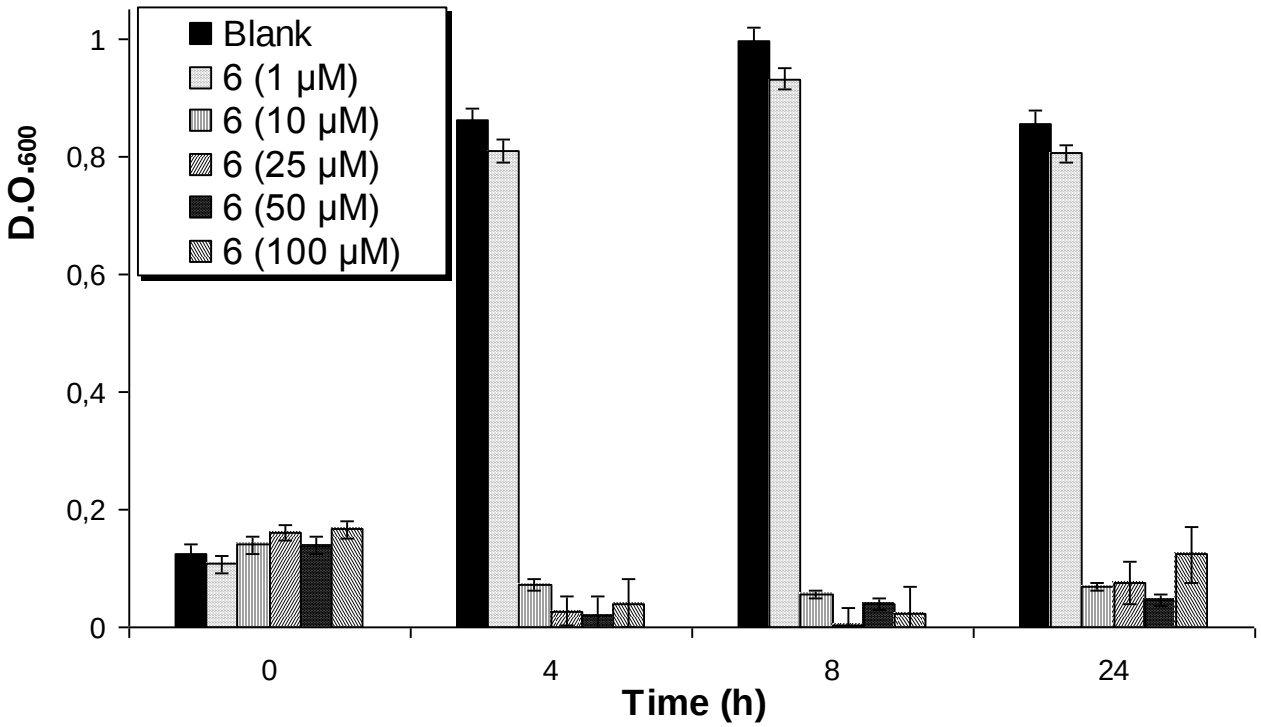

Supplementary figure S56. Dose-dependent growth inhibition of *B.thuringiensis (HD73)* by **6**.

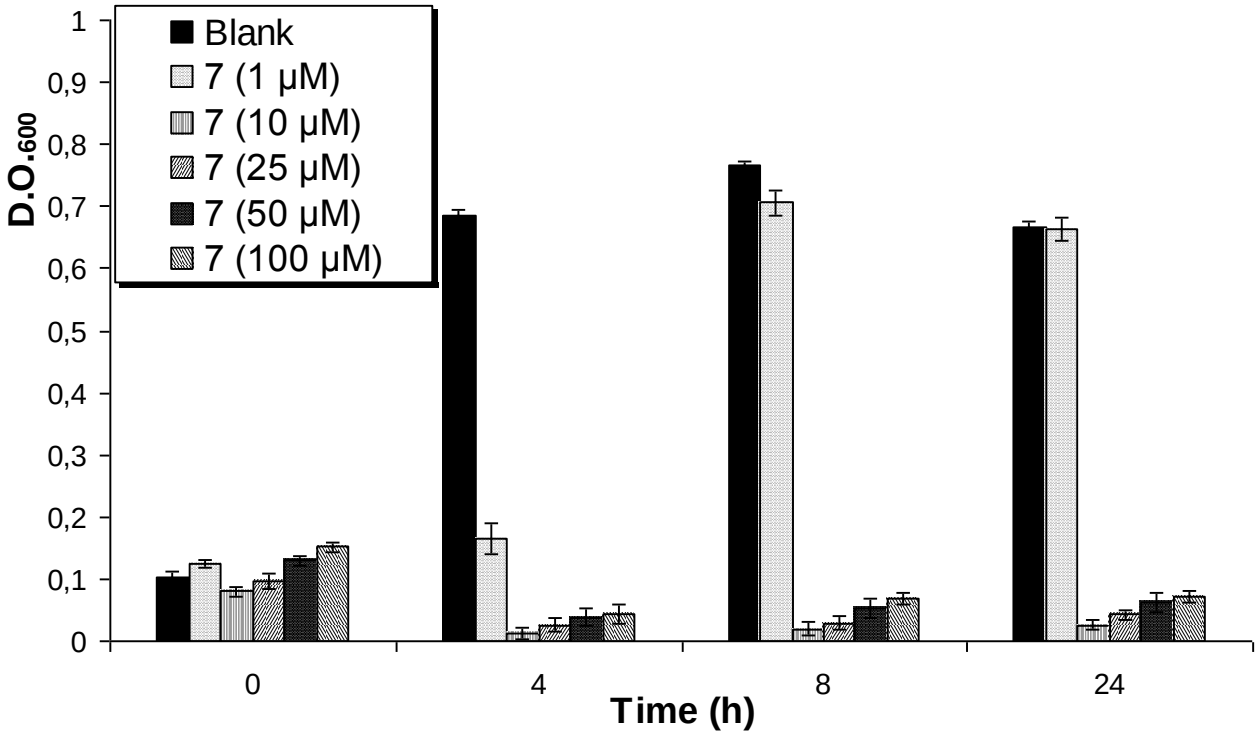

Supplementary figure S57. Dose-dependent growth inhibition of *B.thuringiensis (HD73)* by **7**.

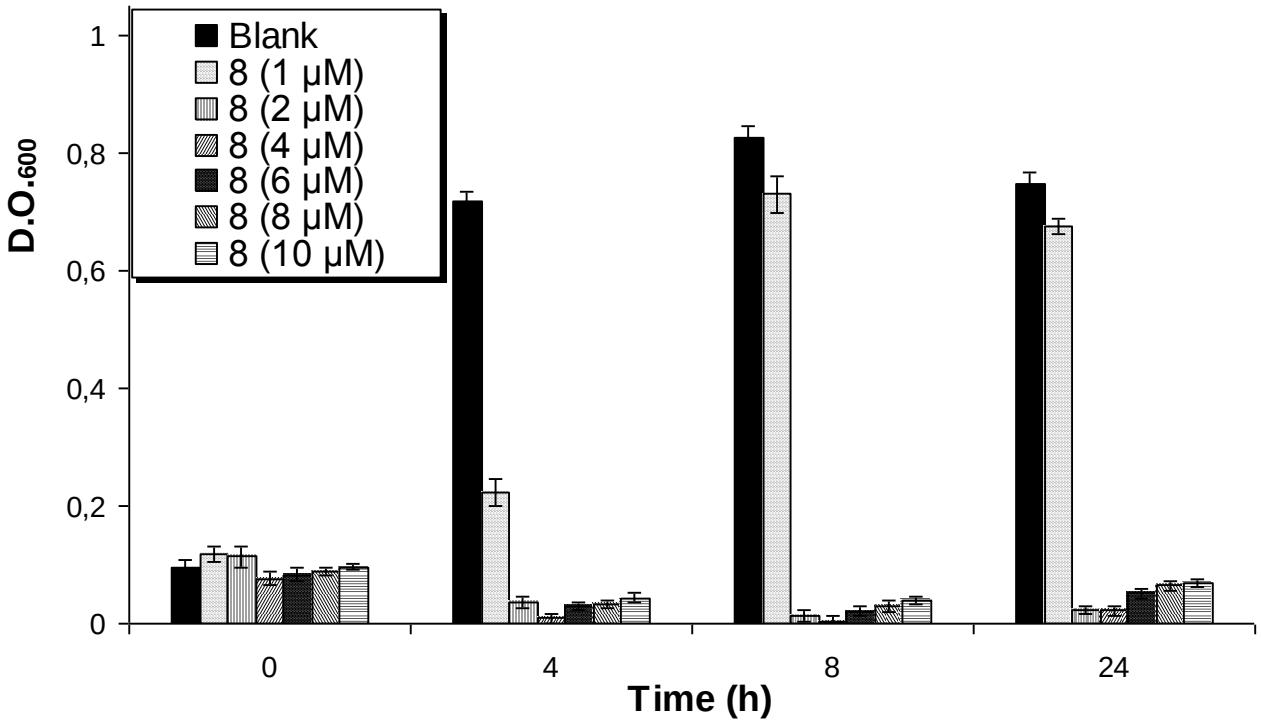

Supplementary figure S58. Dose-dependent growth inhibition of *B.thuringiensis (HD73)* by **8**.